Mercury at the Oat Hill Extension Mine and James Creek, Napa County, California: Tailings, Sediment, Water, and Biota, 2003-2004

By Aaron J. Slowey,[1] James J. Rytuba,[2] Roger L. Hothem,[3] and Jason T. May[4]

2007

Open File Report 2007-1132

[1] Research Chemist, Geology Discipline, 345 Middlefield Rd, MS 901, Menlo Park, California 94025; aslowey@usgs.gov; 650 329-5474.

[2] Research Geologist, Geology Discipline, jrytuba@usgs.gov

[3] Research Wildlife Biologist, Biology Discipline, roger_hothem@usgs.gov

[4] Aquatic Ecologist, Water Resources Discipline, jasonmay@usgs.gov

U.S. Department of the Interior
U.S. Geological Survey

U.S. Department of the Interior
DIRK KEMPTHORNE, Secretary

U.S. Geological Survey
Mark D. Myers, Director

U.S. Geological Survey, Menlo Park, California 2007

For product and ordering information:
World Wide Web: http://www.usgs.gov/pubprod
Telephone: 1-888-ASK-USGS

For more information on the USGS—the Federal source for science about the Earth, its natural and living resources, natural hazards, and the environment:
World Wide Web: http://www.usgs.gov
Telephone: 1-888-ASK-USGS

Suggested citation:
Slowey, A.J., Rytuba, J.J., Hothem, R.L., May, J.T., 2001, Mercury at the Oat Hill Extension Mine and James Creek, Napa County, California: Tailings, sediment, water, and biota, 2003-2004: U.S. Geological Survey Open-File Report 2007-1132, 60 p.
[http://pubs.usgs.gov/of/2007/1132/]

Contents

List of Tables

List of Figures

Executive Summary

The Oat Hill Extension (OHE) Mine is one of several mercury mines located in the James Creek/Pope Creek watershed that produced mercury from the 1870's until 1944 (U.S. Bureau of Mines, 1965). The OHE Mine developed veins and mineralized fault zones hosted in sandstone that extended eastward from the Oat Hill Mine. Waste material from the Oat Hill Mine was reprocessed at the OHE Mine using gravity separation methods to obtain cinnabar concentrates that were processed in a retort. The U.S. Bureau of Land Management requested that the U.S. Geological Survey measure and characterize mercury and other chemical constituents that are potentially relevant to ecological impairment of biota in tailings, sediment, and water at the OHE Mine and in the tributaries of James Creek that drain the mine area (termed *Drainage A* and *B*) (Figs. 1 and 2). This report summarizes such data obtained from sampling of tailings and sediments at the OHE on October 17, 2003; water, sediment, and biota from James Creek on May 20, 2004; and biota on October 29, 2004. These data are interpreted to provide a preliminary assessment of the potential ecological impact of the mine on the James Creek watershed.

The mine tailings are unusual in that they have not been roasted and contain relatively high concentrations of mercury (400 to 1200 ppm) compared to unroasted waste rock at other mines. These tailings have contaminated a tributary to James Creek with mercury primarily by erosion, on the basis of higher concentration of mercury (780 ng/L) measured in unfiltered (total mercury, Hg_T) spring water flowing from the OHE to James Creek compared to 5 to 14 ng/L Hg_T measured in James Creek itself. Tailing piles (presumably from past Oat Hill mine dumping) near the USBLM property boundary and upstream of the main OHE mine drainage channel (*Drainage A*; Fig. 2) also likely emit mercury, on the basis of their mercury composition (930 to 1200 ppm). The OHE spring water is likely an appreciable source of sulfate and carbonate to

James Creek, because the spring water was enriched in sulfate (130 mg/L) and carbonate (430 mg/L as $CaCO_3$) compared to James Creek water (70 to 100 mg/L SO_4^{2-} and 110 to 170 mg/L as $CaCO_3$) at the time of sampling. Concentrations of mercury in active channel sediment from James Creek are variable and potentially high, on the basis of chemical analysis (2.5 to 17 μg/g-wet sediment) and easily visible cinnabar grains in panned concentrates.

Average (geometric mean) organic mercury (presumably monomethyl mercury (MMHg); §2.3.3) concentrations in several invertebrate taxa collected from the James Creek watershed locations were higher than invertebrates taken from a Northern California location lacking a known point source of mercury. The mean proportion of MMHg to total mercury in James Creek predatory insect samples was 40 percent (1 standard deviation = 30 percent); only 40 percent of all insect samples had a $MMHg/Hg_T$ proportion greater than 0.5. The low proportions of MMHg measured in invertebrates in James Creek and the presence of cinnabar in the creek suggest that some invertebrates may have anomolously high Hg concentrations as a result of the injestion or adhesion of extremely fine-grained cinnabar particles.

Interpretation of Hg_T in frogs and fish as an indicator of mercury reactivity, biouptake, or trophic transfer is limited, pending MMHg measuremens, by the possibility of these whole-body samples having contained cinnabar particles at the time of analysis. To minimize this limitation, the gastrointestinal tracts and external surfaces of all amphibians, where cinnabar most likely resides, were carefully flushed to remove any visible particles. However, extremely fine-grained, invisible, adhesive cinnabar particles likely exist in the amphibians' habitats.

Hg_T in foothill yellow-legged frogs collected from the James Creek study area, ranging from 0.1 to 0.6 μg/g Hg, was on average twice that of an extensive database compiled from Hg_T in frogs studied throughout Northern California. Average concentrations of Hg_T in frogs from James Creek were similar upstream (0.18 μg/g) and downstream (0.15 μg/g) of the confluence with Tributary 1 and at the lower Corona Mine adit drainage (0.14 μg/g). Frogs may be susceptible to trophic transfer of MMHg from invertebrates, but further study is required to rule out cinnabar 'contamination.'

Hg_T concentrations in rainbow trout collected from James Creek upstream and downstream of Tributary 1 averaged 0.10 μg/g and 0.13 μg/g, respectively. Compared to invertebrates, trout Hg_T was less variable, suggesting that trout were less contaminated with cinnabar. California roach had significantly higher Hg_T on average than trout (0.16 vs. 0.12 μg/g), and can be considered moderately contaminated compared to the same species from other sites in Northern California, which average 0.12 μg/g Hg.

While limited measurements of mercury in water, sediment, and fish exceed, in some samples, predefined ecologically protective criteria for mine-impacted California systems, they do not clearly demonstrate that the biota residing in James Creek in the vicinity of the OHE are ecologically impaired. The potential for ecological impairment is clearly evident from invertebrate methyl mercury results and may manifest in other biological ecosystem residents that have yet to be studied (e.g., piscivorous birds). Methyl mercury concentrations in flowing water and sediment from James Creek and the tributary that drains the OHE are relatively low, ranging from 0.04 to 0.08 ng/L, although these data should be cautiously interpreted (see § 3.2).

While the results of this investigation suggest that the OHE contributes inorganic mercury to James Creek, they do not indicate the extent to which the OHE site is ecologically impairing biota relative to other sources of mercury. Improved sampling and analytical methods are recommended for future study.

1. Introduction

1.1 Background

The Oat Hill Extension (OHE) Mine is one of several mercury mines in the East Mayacamas mining district that produced mercury from the early 1870s until 1944 (U.S. Bureau of Mines, 1965). This mine produced an estimated 1,000 flasks of mercury, whereas the larger neighboring Oat Hill Mine produced 165,000 flasks of mercury over a similar period. The Oat Hill and nearby Corona and Twin Peaks mercury mines are located on private land in the upper part of the James Creek watershed (Fig. 1, appended). The OHE is located on federal land managed by the U.S. Bureau of Land Management (USBLM). The USBLM requested that the U.S. Geological Survey (USGS) measure and characterize mercury and other chemical constituents in tailings, sediment, water, and biota at the OHE Mine and the tributary of James Creek that drains the mine area (Fig. 2, appended) relevant to recognizing impairment of biota. This report summarizes data obtained from sampling of tailings and sediments at the OHE on October 17, 2003; water, sediment, and biota from James Creek on May 20, 2004; and biota on October 29, 2004. These data are interpreted to provide a preliminary assessment of the potential ecological impact of the mine on the James Creek watershed.

1.2 Geology and Mining History

The mercury ores in the Mayacamas mining district occur in greywacke (sandstone) of the Franciscan Formation at the Oat Hill and OHE mines, and in silica-carbonate altered serpentinite at the Corona and Twin Peaks mines. The sandstone has been hydrothermally altered primarily to kaolinite and quartz in the mineralized area. Cinnabar (alpha-HgS) is the primary ore mineral and usually occurs in association with pyrite (FeS_2). Calcite and quartz veins are present in the altered sandstone and locally contain cinnabar. Elemental sulfur is present in the upper part of the Oat Hill deposit that, along with kaolinite alteration, indicates that the mercury was deposited in the steam-heated environment above the paleo-groundwater table.

Mercury ores at the OHE mine were mined from the eastern extension of veins and mineralized fault zones of the Oat Hill mine. Thus, the ore grades were likely similar at both mines, although specific information for ore grades at the OHE are not available. Ore grades at the Oat Hill mine ranged from 0.75 to 1.0 percent, with grades as high as 2 percent during the early years of mining. Because of poor mercury recovery from the ore, both the waste rock and tailings, containing as much as 0.16 percent mercury, were locally reprocessed at both the Oat Hill and OHE Mine.

Material from mine waste piles was brought from the Oat Hill mine to the OHE property and reprocessed using a trommel (rotating sieve) and concentrating tables. During this concentration process, oversized fragments from the trommel were discarded to a waste pile and undersized fragments[1] were sent to a concentrating table where the cinnabar was removed, and the waste sent to a tailings pile (Fig. 3) (U.S. Bureau of Mines, 1965). Because the material was not processed in a retort or furnace, the tailings from this process are unusual. Only the cinnabar

[1] There is no record indicating that additional crushing occurred prior to cinnabar removal.

concentrate was processed in a one-pipe retort (Fig. 4). As a result, only a minimal amount of calcine generated from the retort was disposed of in the tailings pile.

Figure 3. Overview of tailings pile at the Oat Hill Extension. Note drainage channel containing barrels in central part of photo is shown in detail in Figure 12.

Mercury contamination of James Creek by cinnabar from the Oat Hill and OHE mines is substantial. Erosion down steep slopes of waste rock, tailings, and other mine waste at the Oat Hill and OHE seasonally replenished placer cinnabar deposits in James Creek (Yates and Hilpert, 1946). Some of the cinnabar from these deposits was recovered using a rocker (Fig. 5) and other placer mining techniques within a distance of 3 km downstream from the Oat Hill mine area.

Figure 4. Remains of brick retort at Oat Hill Extension location of sample 23OE11.

1.3 Transport and biogeochemistry of mercury in mine waste-contaminated sediments

The transport of mercury from mercury mine waste materials, including waste rock and calcines, is usually dominated by $HgS_{(s)}$ colloids (Conaway *et al.*, 2004; Kim *et al.*, 2004; Slowey *et al.*, 2005a; Whyte and Kirchner, 2000). In addition, more soluble forms of mercury are released, a fraction of which is adsorbed to particles.[2] During fluvial transport, $HgS_{(s)}$ remains in sediments and soluble mercury may accumulate by binding to organic-rich material in sediments. Investigations at other sites by the authors have found evidence of anaerobiosis where plant roots trap sediment. While plant roots stabilize sediment at these locations, plant litter

[2] Speciation measurements by Kim et al. (2004) of a calcine sample at the Oat Hill mine found it to contain 940 ppm total Hg, consisting of (in order of increasing expected solubility) 60 percent cinnabar (alpha-HgS), 10 percent each of coderoite ($Hg_3S_2Cl_2$) and terlinguite (Hg_2OCl), and 20 percent $HgCl_2$.

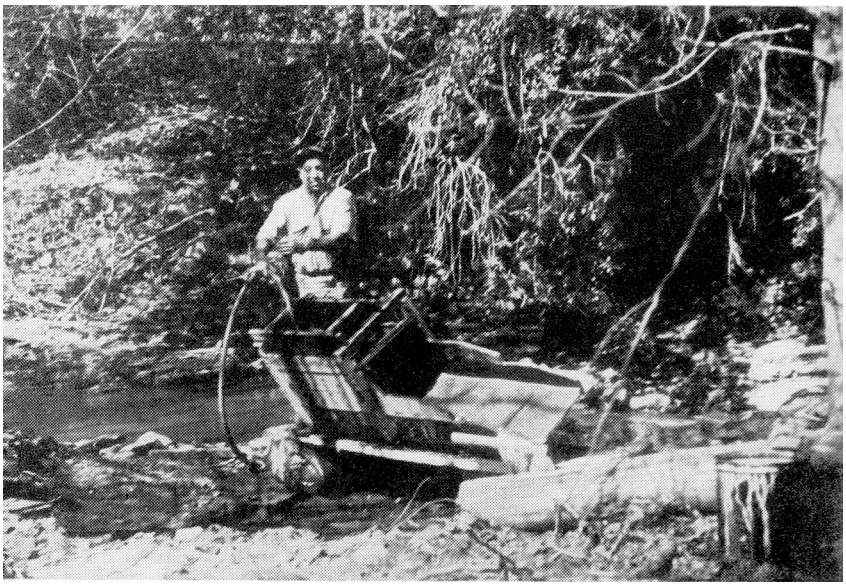

Figure 5. Historic placer mining of cinnabar using a rocker in James Creek below the Oat Hill Mine tailings.

provides organic matter, enhancing microbial activity. In sulfate-rich water, sulfide production has been observed in this type of environment, presumably due to the activity of sulfate-reducing bacteria (SRB). Some *species* of SRB are known to methylate mercury in freshwater sediments (Benoit *et al.*, 2003; Gilmour *et al.*, 1992). The abundant iron present in James Creek[3] also likely affects the transport and biogeo-chemistry of mercury.

Fe(III)-(hydr)oxide formed from pyrite weathering or microbially mediated Fe(II) oxidation is often fine-grained with high surface area (Banfield *et al.*, 2000; Gilbert and Banfield, 2005; Kappler and Straub, 2005; Nordstrom and Southam, 1997). The properties of these types of particles are relevant in at least three respects to the reactivity of inorganic mercury (including its propensity to be methylated):

(1) Hg(II) will adsorb to Fe(III)-(hydr)oxide (Barrow and Cox, 1992),
(2) Fe(III)-(hydr)oxide will readily react with sulfide, and
(3) bacteria can metabolically reduce Fe(III), potentially releasing sorbed Hg(II) into solution.

Some Fe(III)-reducing bacteria have also been found to methylate mercury (Fleming *et al.*, 2006; Kerin *et al.*, 2007). Geochemical reactions between Fe(III)-(hydr)oxide and sulfide appreciably affect the reactivity of $HgS_{(s)}$ under anaerobic conditions, because sulfide oxidation by Fe(III) can result in the formation of polysulfide ions (Poulton *et al.*, 2004; Pyzik and Sommer, 1981; Slowey and Brown Jr., 2007), which can increase the solubility of $HgS_{(s)}$ by up to three orders of magnitude (Jay *et al.*, 2000; Paquette and Helz, 1997) and make more mercury (initially as aqueous Hg(II)-polysulfide complexes) available for methylation (Benoit *et al.*, 2001; Jay *et al.*, 2002). The aqueous chemistry of polysulfide has been studied more to understand the diagenesis of iron and sulfur in sediments (Rickard and Morse, 2005).

Estimating the methylation potential of a system that has an abundant source of inorganic mercury such as James Creek is limited in part by the extent to which potentially relevant biogeochemical processes have been investigated and understood. Discussion of the results of

[3] Since 2003, reductions in discharge of iron (hydr)oxide from the Twin Peaks and Corona mine sites through trench and settling basin construction has noticably reduced the amount of iron (hydr)oxide in James Creek, based on observations in January and March, 2007.

this investigation explains how a sampling program may under-represent methylation potential in the absence of information on biogeochemical processes associated with methylation.

2. Sample Locations and Methods

2.1 Sample Locations and conditions

Samples were collected to assess the concentration of mercury and other potentially relevant chemical constituents in tailings at the OHE Mine, and in sediments, waters, and biota in James Creek and the unnamed tributary to James Creek that drains the mine area, here termed *Tributary 1*. Samples of tailings and sediments at the OHE Mine were collected on October 17, 2003. Water, sediment, and biota from James Creek and Tributary 1 were sampled on May 20, 2004, during early summer base stream-flow conditions. Flow measurements were not made at the time of sampling and, to our knowledge, no gage is present in the James Creek watershed. During both sampling times, the weather was stable and no precipitation occurred. Field sites are shown on Figure 1 and 2 and listed and described in Table 1. The geographic coordinates in Table 1 were obtained in the field using a hand-held global positioning system referenced to the NAD 27 datum.

Table 1. Sample locations and descriptions. See Fig. 1 and 2 for maps illustrating these locations and their hydrological relationship. Coordinates are based on the NAD 27 datum.

Sample[1]	Latitutde	Longitude	Description
04JC1	38.66965	122.5178	James Creek above confluence with Oat Hill Extension drainage (*Tributary* 1).
04JC2	38.67013	122.5142	Tributary 1 at confluence with James Creek.
04JC3	38.66988	122.5127	James Creek water below confluence with Tributary 1.
04OHE1(S)	38.67857	122.5177	OHE drainage (Drainage B) to Tributary 1 (spring water).
23OE12	38.67910	122.51814	OHE tailings above adit (upper tailings)
23OE13S	Near OE12		Sediments near upper tailings
23OE1 through 9	Near OHE1		OHE tailings or, with an 'S' suffix, sediments
23OE11	Near OHE1		Sample of retort brick
23OE14	38.67752	122.51819	OHE office site (background soil sample)
CRN-D/U	38.67077	122.5369	James Creek up & down-stream of lower Corona Mine adit

Notes: (1) 04 indicates samples taken in 2004; JC = James Creek; OHE = Oat Hill Extension Mine site.

2.2 Sampling

2.2.1 Dry sediment and tailings

Visually representative, 100 to 500 g samples of tailings were collected from the OHE tailings pile after removing the upper 2 cm of exposed tailings. Tailings were also sampled along Drainage A where exposed in vertical sections along the channel. Up to 500 g of air-dried tailings were placed in trace-metal free certified borosilicate glass jars with Teflon-lined caps (I-CHEM Series 300). Grab samples of dry sediment consisting primarily of transported tailings (on the basis of visually similar composition and grain size) were similarly collected and stored. Most sediment clasts larger than coarse sand size (2 mm) were discarded.

2.2.2 Wet sediment and tailings

Grab samples of wet sediments were collected for total mercury (Hg_T) and monomethyl mercury (MMHg) analysis at three James Creek locations and in Tributary 1 (Figs. 1 and 2). On May 20, 2004, sediment samples, which consisted of silt and fine to medium sand-size particles, were taken from the active channel of the creek into 100-mL polycarbonate jars. Samples were stored in coolers with ice immediately after collection and frozen upon return from the field within four hours after collection until shipped to the analytical laboratory. Samples were shipped with blue ice packs and arrived at the analytical lab at 15ºC, which is warmer than recommended for MMHg analysis (Bloom, 2001; USEPA2002). Once at the laboratory (May 24, 2004), sediment samples were frozen again until processed.

2.2.3 Water

Spring and stream water samples were collected with new 60-mL sterile polypropylene syringes at the same time as sediments were collected on May 20, 2004. Bulk water samples were subsampled for analysis of metals and metalloids [to be referred to hereafter using the shorthand metal(loid)s] and anions. Subsamples for metal(loid)s determinations were acidified to pH<2 with trace metal (*Ultrex*, J.T. Baker)-grade HNO_3 and stored in acid-washed, high-density polyethylene (HDPE) bottles. Subsamples for anion and alkalinity measurements were filtered, stored in HDPE bottles, and chilled to approximately 4°C until analysis, in accordance with U.S. Geological Survey protocols (http://pubs.water.usgs.gov/twri9A). Water samples for analysis of anions alkalinity, and ICP-MS and ICP-AES analysis were filtered in the field with 0.45 μm, 25-mm sterile cellulose acetate syringe filters. Field method blanks were collected for one site by processing deionized water according to the same procedures used for field samples (except for alkalinity).

Water parameters including pH, conductivity, and temperature were measured in the field with a Orion Model 290 pH meter equipped with a temperature-compensated electrode and an Orion Model 120 conductivity meter.

Samples for Hg_T and MMHg analyses were obtained separately from the same location in James Creek and Tributary 1 in 1-L borosilicate bottles with no headspace using Teflon-lined caps (I-CHEM Series 300) following ultra-clean sampling and handling protocols (Bloom, 1995). Samples were kept on ice at approximately 5°C until analysis.

Figure 6. James Creek location JC1 upstream of OHE drainage sampled for biota in Spring and Autumn 2004.

Figure 7. James Creek location JC3 downstream of Oat Hill Extension mine drainage sampled for biota in Spring and Autumn 2004.

2.2.4 Biota

Biological samples were collected from five sites in the James Creek watershed at the Oat Hill Extension mine area based on suspected Hg contamination and the presence of appropriate study organisms. Locations on James Creek upstream (JC1), above the confluence (JC2), and downstream (JC3) of Tributary 1 (Figs. 2, 6, and 7) and a small wetland area formed by a spring at location OHE1 (Figs. 1, 2 and 9) were sampled along with water and sediment on May 20, 2004. JC1, JC3, OHE1 and a location where lower Corona Mine[4] adit drainage enters James Creek at the base of Kidd Canyon were sampled on October 29, 2004 (location CRN, Figs. 1 and 10).

Target macroinvertebrates for this study were predatory aquatic insects, collected depending on their abundance and availability at sampling sites. Preferred macroinvertebrates included: dragonflies (Odonata, families Gomphidae, Cordulegastridae, and Aeshnidae), beetles (Coleoptera, family Dyticidae, predaceous divingbeetles), aquatic and semi-aquatic predaceous insects of the order Hemiptera (family Gerridae, water striders; family Notonectidae, back swimmers; family Belostomatidae,giant water bugs), stoneflies (Plecoptera, family Perilidae), and dobsonflies (Megaloptera, family Corydalidae). Water striders are surface, not sediment feeders. Giant Waterbugs are of the same order (Hemiptera) as water striders, and similar to the striders, feed with piercing sucking mouthparts. However, they are not surface feeders like water striders, but feed within the water column and sediments. Dragonflies, dobsonflies, beetles, and stoneflies are benthic invertebrates and feed in sediment. Invertebrates were collected using dip nets or by hand, placed in zip-lock plastic bags with native water, kept on wet ice, and sorted at the end of each day.

Individual invertebrates were sorted by family and placed in disposable dishes using Teflon-coated forceps or a gloved hand. Organisms were thoroughly rinsed with deionized water and patted dry with clean paper towels. Up to 30 individuals of the same family were composited into 0.5 to 3 g samples in clean glass jars with Teflon-lined lids and frozen until shipped to the laboratory for analysis for total mercury and methyl mercury.

[4] Speciation measurements by Kim et al. (2004) of condenser soot at the Corona Mine found it to contain 550 ppm total Hg, consisting of 50 percent cinnabar (alpha-HgS), 40 percent metacinnabar (beta-HgS), and 10 percent schuetteite ($Hg_3O_2SO_4$). Reductions of mercury transport achieved by recent construction of settling basins to intercept Corona Mine drainage have yet to be documented.

Figure 8. Sampling location JC2 on Tributary 1, spring 2004. The drain was dry in the Autumn sampling period, and no samples were collected.

Foothill yellow-legged frogs (*Rana boylii*) were captured by hand or with a net during the day: five in May and two in October, 2004. Foothill yellow-legged frogs appeared to be relatively abundant in James Creek in the spring, but few were seen in autumn of that year. Frogs were individually placed in plastic bags on wet ice, humanely euthanized with MS-222 the same day they were collected (American Society of Ichthyologists and Herpetologists et al., 1987), and frozen until processed within 2 days after collection.

Clean tools, weigh dishes, and disposable latex gloves were used to process each frog specimen to avoid cross contamination. Each frog was thawed, rinsed first with tap water to remove debris and then with deionized water, patted dry, and weighed ($\pm$ 0.1 g). The snout-vent length (SVL) was measured using calipers ($\pm$ 0.1 mm), and we examined each specimen for gross abnormalities. The digestive tract was removed, and the carcass, including the stripped and rinsed digestive tract, was placed in a clean jar (VWR TraceClean), sealed with Parafilm, and frozen at –20º C pending chemical analysis for total Hg.

Rainbow trout (*Oncorhynchus mykiss*) and California roach (*Hesperoleucus symmetricus*) were collected from the two James Creek sites (JC1 and JC3; Fig. 1) in spring of 2004 using a backpack electroshocker. Similar sizes and species were collected at each site as much as possible. Captured fish were held in buckets with native water and then euthanized. Each fish was weighed using an electronic balance ($\pm$ 0.1 g), measured using a measuring board ($\pm$ 0.1 mm) for 'standard' and 'total' length, individually wrapped in aluminum foil, placed in zip-lock bags, and placed on wet ice in a cooler. 'Standard' length is defined as the distance from the tip of the closed mouth to the posterior end of the caudal peduncle, whereas 'total' length is the distance from the closed mouth to the extreme tip of the caudal fin. Samples were stored frozen until they could be processed. In the laboratory, individual fish were examined for gross deformities, dissected to determine sex, and the gastrointestinal tract removed and foods preserved for later identification. Carcasses, less the food contents, were stored frozen in chemically cleaned jars for later analysis for total mercury.

Figure 9. Wetland area near Oat Hill Extension Mine (OHE1, Fig. 2) sampled for biota in Spring and Autumn 2004.

2.3 Analytical Methods

2.3.1 Sediment and tailings

Multi-element analyses for all tailings and dry sediments were performed in the laboratories of ALS Chemex (Reno, NV). Bulk samples were ground in a zirconia ring mill and subjected to a near-total four-acid digestion. Major elements were determined by inductively coupled plasma-atomic emission spectroscopy (ICP-AES). Trace elements other than mercury were determined by inductively coupled plasma–mass spectrometry (ICP–MS). Mercury was determined by cold vapor atomic absorption spectroscopy (CVAAS) following methods similar to those described by Crock (1996) and O'Leary and others (1996).

Mercury and MMHg analyses of wet sediments were carried out by Brooks Rand (Seattle, WA). Sediment subsamples were not homogenized prior to analysis. For total mercury, approximately one gram of sediment was digested with 7 mL conc. nitric acid plus 3 mL conc. sulfuric acid and heated to 100°C for one hour, followed by refluxing at 150°C for two hours in a glass vial with Telon-lined lids. BrCl was added to the digestate after it had cooled to room temperature, diluted to 40 mL with deionized water, further diluted by 40 to 100-fold (such that the concentration was within instrumental range), and followed by stannous chloride reduction, single-stage gold amalgamation, and cold vapor atomic fluorescence spectroscopy (CVAFS) (U.S. EPA Method 1631E). The acid digestion procedure should recover elemental, adsorbed, and almalgamated mercury, and mercury sulfide ($HgS_{(s)}$, including cinnabar and metacinnabar), but does not appreciably dissolve silicate minerals.

Figure 10. James Creek site downstream of lower Corona Mine adit (Fig. 1) sampled for biota in Autumn 2004.

Previous studies suggest that mercury is sorbed to aluminosilicate minerals that exist in fluvial sediment such as those studied here, but only minor fractions of mercury have been found within aluminosilicate mineral structures (Lowry *et al.*, 2004; Slowey *et al.*, 2005b). MMHg in sediment was determined by acid bromide-methyl chloride extraction, followed by aqueous phase ethylation, isothermal gas chromatographic separation, and CVAFS detection (Horvat *et al.*, 1993b). Results are reported on both a wet- and dry-weight basis, with the latter calculated from wet concentrations and gravimetrically measured sediment water contents. Detection limits for Hg_T and MMHg in sediment were 0.12 ng/g and 0.02 ng/g, respectively, representing three standard deviations above mean values derived from multiple analyses of blanks. NIST-certified mercury standard reference materials were measured, including MMHg standards made from pure powder and calibrated against NBS-3133, and cross verified by daily analysis of Certified Reference Material DORM-2 (National Research Council of Canada Institute for National Measurement Standards, 1999).

2.3.2 Waters

Alkalinity was measured two to four days after sample collection by titration with sulfuric acid using Gran's technique (Rounds, 2006). Sulfate, chloride, nitrate, and fluoride were determined by ion chromatography (Fishman and Friedman, 1989). Cations were analyzed by ICP–AES and ICP–MS. Duplicate water samples, blank samples, and USGS Water Resource Division standard reference waters were analyzed with the data set and yielded acceptable results.

Samples for Hg_T and MMHg analyses were handled in a Class-100 clean-air station to minimize sample contamination (Brooks Rand, Seattle, WA). Hg_T was measured by bromine monochloride (BrCl) oxidation followed by $SnCl_2$ reduction, single-stage gold amalgamation, and detection by CVAFS (EPA Method 1631Bloom *et al.*, 1988). MMHg was analyzed using aqueous phase ethylation with purging onto Carbotrap, gas chromatographic (GC) separation, isothermal decomposition, and CVAFS detection (Horvat *et al.*, 1993a). Detection limits for Hg_T and MMHg in water were 0.2 ng/L and 0.04 ng/L, respectively, based on three standard deviations above mean values for multiple blanks.

2.3.3 Biota

All samples collected in May were analyzed by the Trace Element Research Laboratory (TERL, College Station, TX), while the samples collected in October were analyzed by Brooks Rand (Seattle, WA). At Brooks Rand, for Hg_T, samples were digested in a mixture of nitric and sulfuric acid and then oxidized with BrCl, and the digestates analyzed for Hg_T as explained in section 2.3.2. At Brooks Rand, for MMHg, samples were digested in KOH-methanol solution, and the digestates analyzed for MMHg as explained in section 2.3.2. Moisture content was determined by weight loss upon freeze-drying and was expressed as a percent of the original wet sample weight. Mercury and MMHg concentrations are reported on a wet-weight basis.

At TERL, tissue samples were homogenized in the original sample containers either after freeze-drying or with a Tekmar Tissumizer and subsampled. Subsamples were digested with nitric acid, sulfuric acid, potassium permanganate, and potassium persulfate in polypropylene tubes in a water bath at 90-95° C, according to a modified version of EPA methods 245.5 and 245.6. Before total Hg analysis, hydroxylamine hydrochloride was added to digestates to reduce excess permanganate. Digestates were brought to volume with deionized water and analyzed using

Figure 11. Exposure of coarse grained tailings at the lower part of the Oat Hill Extension tailings pile, site of sample 23OE1. Tailings appear to be coated by white efflorescent salts.

stannous chloride reduction, purging and cold-vapor atomic absorption spectroscopy (CVAAS) detection.

Determination of methylmercury in biota was based on extraction of organo-mercury compounds at TERL following the method of Uthe et al. (1972). Organic mercury compounds were extracted from homogenized tissue aliquots using an organic solvent amended with potassium bromide and copper sulfate to improve partitioning from the aqueous to the organic phase. The organic phase was digested in combusted glass vials using nitric and sulfuric acids and potassium permanganate, to convert all Hg species to ionic Hg(II) and to remove traces of organic solvent that would otherwise affect the measurement. The digestates were finally analyzed by CVAAS.

2.4 Geochemical Modeling

A thermodynamic model was used to compare ion activity products of major elements in James Creek water and OHE drainage to the solubility of minerals that may precipitate and dissolve

under low-temperature aqueous conditions. The computer program Geochemist's Workbench (version 6) estimated activities from concentrations using a modified form of the "B-dot" equation (Helgeson, 1969) and computed the saturation index, S.I. = Q/K, for minerals contained in the 'thermo.dat' database (http://www.geology.uiuc.edu/Hydrogeology/hydro_thermo.htm), where Q is the ion activity product of a given mineral's constituents (e.g., Mg^{2+} and CO_3^{2-} for magnesite) and K is the solubility product of that mineral. Calculations used a constituent basis estimated from water quality (temperature, pH, and alkalinity) and aqueous constituent measurements, included a fixed sea-level atmospheric oxygen fugacity of 0.2 (approximately 10 mg/L dissolved oxygen), and took ion-pairing into account.

3. Results

3.1 Tailings and Dry Sediment at OHE Mine

Ore processing at the Oat Hill Extension (OHE) resulted in significant residual cinnabar and pyrite in the tailings. The OHE mill feed, consisting of sandstone and former tailings from the Oat Hill Mine operation, was gravimetrically separated but not heated. This method is in contrast to the more typical process of roasting, which would have removed more mercury and oxidized minerals such as pyrite. Waste pile tailings are stratified based on clast size, apparently ranging

from coarse sand to coarse gravel (Fig. 11). The coarser tailings occur in the northern part of the pile (sample 23OE9; Fig. 2), and reflect accumulation of oversize clasts rejected from the trommel. Tailings in the southern part of the pile, samples 23OE1 through 5 (Fig. 2), consist primarily of undersize clasts rejected from the concentrating tables.

The geochemical results for samples of mill tailings at the OHE are listed in Table 2 (appended). The mercury concentrations in the tailings range from 400 to 1000 μg/g (ppm). Tailings present above the adit in the northern-most part of the mine area, sample 23OE12 (Fig. 2), have the highest concentration of mercury (1175 ppm). Other potentially toxic metal(oid)s are present at lower concentrations, including arsenic (0.2-6 ppm), copper (30-50 ppm), nickel (50-70 ppm), lead (10-20 ppm), and zinc (90-130 ppm) (discussed further below).

Background soil sampled at the OHE at a distance of 0.5 km from the retort site has a mercury concentration of approximately 7 ppm (23OE14; Fig. 2). The high level of mercury in the soil is either due to mercury mineralization of the sandstone from which the soil developed or atmospheric deposition following emission from retort and furnace stacks at the Oat Hill and

adjacent Corona and Twin Peaks mine sites (Ericksen *et al.*, 2005; Gustin *et al.*, 2003; Gustin *et al.*, 2004). Further soil sampling is required to evaluate disseminated mineralization and furnace emissions as sources of mercury to the James Creek area.

Elevated mercury concentrations exist in sediment sampled from a channel that transects the upper and lower part of the tailings, here termed *Drainage A* (Fig. 2). The mercury concentration of sediment in the upper part of Drainage A is 930 ppm (sample 23OE13S), increasing to 1500 ppm (sample 23OE3S) in the lower part of the drainage where it incises the main tailings pile (Figs. 2 and 12). Since the 'upper tailings' piles (location 23OE13S) apparently contain high concentrations of mercury, a portion of the mercury in sediment sampled downstream at location 23OE3S could have come from the 'upper tailings' piles. However, since the downstream sample site is located at the tail-end of the OHE tailings piles, the mercury measured in the sediment there could have originated from the OHE tailings alone or from both the OHE tailings and contaminated sediment originating from the 'upper tailings.' That the mercury concentration measured at the downstream location was higher than at the 'upper tailings' location could suggest that mercury is released from the 'upper tailings,' transported down to the OHE site, and mixed with OHE tailings-contaminated sediment in such a way that the mercury concentration is augmented, and then finally discharged at the tail-end of the OHE. Since mercury does not transport conservatively, and in the absence of any hydrological information, the hypothesis stated above cannot be resolved by this simple comparison. Even this small region would require a detailed (e.g., including suspended solids concentrations under different flow regimes), high-resolution characterization to determine from where and in what quantities mercury originates.

Drainage A was dry at the time of sampling, but intense rain in winter probably transports mercury-enriched sediment from the tailings pile into Tributary 1 and then James Creek. The data are consistent with the hypothesis that winter runoff from the Oat Hill and OHE areas replenishes cinnabar in the James Creek placer (Yates and Hilpert, 1946).

Figure 12. Sediment in Drainage A located in the lower part of Oat Hill Extension tailing pile.

Concentrations of mercury, copper, lead and zinc in the lower tailings pile at the OHE site, two sediment samples from Drainage A from the OHE, and tailings above the adit exceed USBLM Robin Scenario (RS) ecotoxicity screening criteria. In addition, five lower tailings samples, two sediment samples from the OHE drainage ditch, and the 'background' soil sample taken at the OHE office site contained arsenic (As) concentrations exceeding the USBLM's RS ecotoxicity screening criteria. Comparisons of all element concentration results with the USBLM's Human Risk Management Camper Scenario and US Environmental Protection Agency preliminary remediation goals (USEPA-PRG) criteria are provided in Table 2. One OHE tailings contained As and chromium exceeding USEPA-PRG criteria, and all but one sample exceeded the USEPA-PRG thorium criterion. All but two samples (retort brick and background soil) exceed the the USBLM Camper Scenario criterion for mercury. Brick and mortar from the retort used to process cinnabar concentrates from the OHE Mine have a relatively low mercury concentration (5 ppm), although it exceeds the USBLM's RS ecotoxicity screening criterion. Other metals that exceed this criteria for this material include As, Cu, Pb, and Zn (Table 2).

3.2 Water and Sediment in James Creek and the Tributary Draining the OHE Mine

In summarizing our mercury monitoring results, we cite predefined water, sediment, and biota quality criteria to compare our observations with what is currently thought by public agencies to pose ecological risk due to mercury in organisms such as piscivorous fish and birds. In California mine-impacted systems, multiple criteria are used, including concentrations of Hg_T or MMHg in water, sediment, fish, or combinations thereof. As further explained in sections 3.2.1 and 3.3.3, direct comparison of a given mercury concentration with the predefined criterion of similar analyte and medium is inappropriate, because multiple and often undisclosed/implicit assumptions used to derive the criterion do not fully apply to the present case. Although beyond the scope of this report, we note that some predefined criteria also intertwine causal relationships derived from seemingly incompatible conceptual models. Ultimately, we cite these predefined criteria to promote awareness and further elucidate the limitations of both the current data set and the criteria themselves.

3.2.1 Mercury and monomethyl mercury

Water and sediment were sampled from a tributary that drains the OHE Mine area (termed *Tributary 1*), and in James Creek in order to assess whether mercury and associated elements were being transported from the mine site into James Creek. In Tributary 1 water just above the

confluence with James Creek, the Hg_T concentration was 14 ng/L (sample 04JC2, Table 3). In James Creek, Hg_T concentrations below this confluence was 55 percent higher than above (7.3 *vs.* 4.8 ng/L; sample 04JC3 *vs.* 04JC1; Table 3), suggesting that mercury is transported through Tributary 1 to James Creek under base flow conditions. Filtered mercury concentrations in Tributary 1 and James Creek waters account for 50 to 60 percent of Hg_T. Drainage from a spring located below the adit of the OHE Mine (termed *Drainage B*; Fig. 2) is an important source of mercury to Tributary 1, since it contains an exceptionally high 770 ng/L Hg_T (sample 04OHE1; Table 3). The water from this spring deposits calcite and magnesite, on the basis of visual observation of the sediment in the spring area and thermodynamic calculations (§3.2.2). This deposition may enhance the accumulation of mercury in OHE drainage sediment (110 μg/g-dry was measured in sample 04OHE1; Table 3).

MMHg concentrations in waters of James Creek and Tributary 1 (0.04 to 0.08 ng/L) are lower than those typical for mine impacted watersheds (~0.1 ng/L; Krabbenhoft *et al.*, 1999), but are near or above a proposed level (0.04 to 0.06 ng/L MMHg on an annual-averaged basis of undefined statistical population) for the mercury mine-impacted Tomales Bay (Marin County), California watershed (Marshall, 2006)[5]. The spring water with the relatively high Hg_T concentration at the OHE (770 ng/L) had the highest MMHg concentration, 0.09 ng/L, which is more typical of mine impacted waters and yet was only 0.01 percent of Hg_T. Invertebrates from this location also had higher levels of MMHg (section 3.3.1). These results should be interpreted with caution for two reasons: (1) sample storage may have resulted in MMHg degradation prior to analysis (Bloom, 2001; Parker and Bloom, 2005) and, more importantly, (2) the waters were oxygenated and sunlit, which can promote biological and photochemical degradation of MMHg (Benoit *et al.*, 2003; Sellers *et al.*, 1996), reducing the likelihood of measuring all of the MMHg produced in sediment, resulting in an unrepresentative coverage of the system's total methylation potential. This sampling bias results in concentrations that are so small as to be especially prone to error when used to relate water quality to impacts on biota. Pore waters at these sample sites should be analyzed to better assess the methylation potential at each site, as discussed at the end of this section.

Figure 13. James Creek at water, sediment and biota sample site 04JC1. Iron staining on rocks in creek results from precipitation of iron (hydr)oxide from the Corona and Twin Peaks mines.

High concentrations of mercury are present in sediment from the active channel of James Creek (Figs. 2 and 13, sample site 04JC1), indicated by panned concentrates that contain a large amount of cinnabar (Figs. 14) and high concentrations of mercury in

[5] This criterion is accompanied by sediment criteria, which arguably is an example of the use of incompatible conceptual models to derive a mercury concentration-ecological impairment relationship.

sediment (7 to 21 ppm; samples 04JC1 and 04JC3, Table 3). Mercury concentrations in sediment and the amount of cinnabar in the panned concentrate were highest at sample site 04JC1, located above the confluence with Tributary 1 (Fig. 2). Mercury concentrations and the amount of cinnabar in the panned concentrate decrease downstream from the confluence with Tributary 1. Concentrations in Tributary 1 (3 ppm, sample 04JC2), are lower than at both samples sites (04JC1and 04JC3) in James Creek. The data suggest that although Tributary 1 is a source of mercury-enriched sediment to James Creek, more significant sources of mercury-enriched sediment exist upstream of Tributary 1. These results must be qualified using quality control analyses, as follows.

Duplicate matrix spike analyses of total mercury in sediment revealed a heterogeneous distribution of mercury within a given grab sample. Recoveries of mercury from two *un*spiked sample aliquots actually exceeded those of two *spiked* aliquots from the same sample. This result, and the presence of cinnabar in the creek sediments, suggests that subsamples from a given grab sample contain different amounts of cinnabar. Another less likely source of variability may have been inconsistent (i.e., matrix-dependent) and incomplete digestion of mercury (primarily cinnabar).

For these reasons, future sediment investigations should include the following: (1) to determine whether there is a 'nugget effect' due to a heterogeneous distribution of mercury, split large samples into equally sized subsamples (according to mass) and analyze, (2) to prevent exclusion of cinnabar particles when subsampling just prior to analysis (as commonly occurs at commercial laboratories) and to facilitate subsample digestion, thoroughly homogenize (sub)samples, and, (3) to assess which sample size is statistically representative of the bulk sediment volume that one wishes to quantify, analyze a series of samples of increasing size (e.g., 1, 10, 20, 50, 100 mg, etc., each homogenized) taken from the same bulk sediment volume. As sample size increases, the mercury concentrations recovered should converge on a representative value. Ideally, for sediments along a drainage channel, the bulk sediment volumes for which representative sample sizes are determined would adjoin. Practical sampling limitations result in bulk sediment volumes separated in space, with unknown but potentially quantifable implications for the reliability of sediment mercury measurements and the conclusions about mercury transport derived from these data. Despite uncertainty in the concentration of Hg_T in sediments of James Creek and its tributaries, the level of mercury contamination is apparently high compared to criteria developed for total mercury in mine-contaminated sediments elsewhere in California. For example, Tomales Bay (Marin County): 5 μg/g in sediment close to mine waste and 0.5 μg/g further downstream (Marshall, 2006).

MMHg concentrations in sediments were relatively low in comparison to sediments from mine-impacted watersheds, which average 1.9 ng/g (Krabbenhoft et al. 1999). Even in the sediment at the OHE with the highest total mercury concentration, the MMHg concentration was only 0.7 ng/g. In addition to the caveats stated earlier for MMHg in water, one sample from James Creek (04JC2) and another from Drainage B (04OHE1) had MMHg concentrations (Table 3) above the method detection limit (MDL) but below a statistically quantifiable concentration (i.e., 10x MDL), and therefore are of questionable value in examining relationships between MMHg in water and MMHg in biota. Nevertheless, high levels of mercury present in sediment and water at the OHE spring, Tributary 1, and James Creek did not result in correspondingly high

concentrations of MMHg in the apparently aerobic water and sediment sampled. The biogeochemical basis for this observation is discussed below.

Cinnabar is typically more soluble under anaerobic, sulfidic conditions (Jay *et al.*, 2000) or in the presence of humic substances (Waples *et al.*, 2005), neither of which characterize the OHE and James Creek sediments sampled in this investigation. Since cinnabar is probably the dominant mercury species in the sediments, the lack of methylation is likely due to the stability of cinnabar under the conditions sampled. To better evaluate the system's true methylation potential, future investigations of James Creek should locate and enumerate zones of anaerobic sediments and analyze the Hg_T and MMHg contents in pore water at these locations.

To more reliably characterize and compare methylation potential among various sites, sampling procedures that minimize *ex situ* environmental and handling effects are needed. For example, if saturated sediments up- and downstream of a mine tailings pile produce MMHg, sediment porewaters will likely contain higher concentrations of MMHg than overlying water, since MMHg will be dispersed and possibly abiotically and biotically degraded (Benoit *et al.*, 2003) as it transports into the water column. If overlying water is sampled at each location, differences in MMHg concentrations may be due to varying degrees of dispersion and/or degradation, not neccessarily a difference MMHg production.

Figure 14. (a) James Creek at sample site 04JC1. Sediment consists of medium to coarse sand and fine silt to clay sizes, the latter containing iron (hydr)oxides derived from Corona and Twin Peaks mine drainage. (b) Cinnabar present in panned concentrate from this location.

Table 3. Mercury and methyl mercury in water and sediment. Error intervals (2σ of duplicate analyses, or 95 percent confidence level) are reported where they are on the order of the last significant digit.

Sample	Mercury in water[1]		Monomethyl mercury in water[2]		Mercury in sediment[3,6]		Monomethyl mercury in sediment[4]	
	unfiltered	Filtered (<0.45 μm)	Unfiltered	Wt% Solid	μg/g wet	μg/g dry[1]	ng/g wet	ng/g dry[5]
04JC1	4.8 ± 0.9	2.8 ± 0.5	0.04	79	17	21	0.72	0.92
04JC2	14 ± 3	7.8 ± 1.5	0.08	76	2.5	3.3	0.06	0.08
04JC3	7.3 ± 1.4	3.4 ± 0.6	0.04	72	5.0	6.9	0.05	0.07
04OHE1	780 ± 150	5.8 ± 1.1	0.10	57	64[6]	110	0.43	0.74

Notes: Analytical detection limits based on 3σ of reagent blank recoveries were (1) 0.2 ng/L, (2) 0.04 ng/L, (3) 0.12 ng/g, and (4) 0.02 ng/g.

(5) Concentrations on a dry weight basis were computed by dividing the ng/g-wet sediment by the wt-percent solids of the sediment.

(6) Matrix spike recovery was *less* than unspiked recovery, indicating substantial heterogeneity in the distribution of Hg within the sediment sample. The true bulk concentration of this and the other sediment samples may be substantially different than these reported values.

In the current study, these processes could not be evaluated because the MMHg concentrations are so low as to be indistinguishable by biogeochemical interpretation. Minimizing ambiguities of dispersion and degradation through appropriate sampling is the first step towards a more direct evalution of methylation potential. Higher, distinguishable MMHg concentrations, perhaps 1 to 10 ng/L differing by tens of percent, would indicate appreciable differences in MMHg production, pending the development of a statistically based method that accounts for biogeochemical effects (i.e., systematic variability). Differences in MMHg production would further imply differences in the locations' abilities to labilize mercury into forms more reactive than cinnabar. MMHg production differences also likely reflect the activity of bacterial populations that are methylating Hg(II). *In situ* sediment pore water sampling using passive or vacuum membrane samplers [e.g., peepers, 'Rhizon' samplers (Seeberg-Elverfeldt *et al.*, 2005), or other high-resolution devices (Merritt and Amirbahman, 2007; Sigg *et al.*, 2006)] will likely recover higher concentrations of MMHg compared to flowing creek water where MMHg that originated in sediment pore water is dispersed in a demethylating environment. The effect of dispersion is clearly evident when comparing MMHg measurements of field samples versus laboratory sediment incubations (Bloom, 2001). Despite the vastly different MMHg concentrations observed in preserved field samples (to estimate *in situ* MMHg concentrations) and field or laboratory reactors, both are used to infer the degree to which inorganic Hg is susceptible to methylation. More reliable assessment of the propensity for inorganic mercury to be methylated will be achieved by determining MMHg concentrations in field samples obtained directly from potential methylation sites by improved sampling methods such as those above.

Reliable assessment of methylation potential is critical to understanding how and to what extent the inorganic Hg load to the James Creek system impacts biota. Measurements of Hg_T and MMHg in biota in conjunction with water and sediment mercury data limited by sampling deficiencies will fail to achieve this understanding, as will be more apparent after reading section 3.3.

3.2.2 Geochemistry of James Creek water and OHE drainage

The pH of James Creek and OHE drainage is buffered by bicarbonate, resulting in a narrow range of pH 8.2 to 8.4 (Table 4). Chloride concentrations are similar among the tested waters and are lower than sulfate, Mg(II), and Ca(II). Thermodynamically calculated ionic strengths of all sampled waters were lower than expected, primarily due to ion pairing of Mg^{2+} and Ca^{2+} with sulfate (20 to 30 percent of Mg(II) and Ca(II) is in the form of $MgSO_4$ and $CaSO_4$; complete results, including other ion pairs, are provided in Appendix 1). These model results emphasize the importance of taking ion pairing into account when interpreting indirect measurements of ionic strength (e.g., conductivity). Magnesium and calcium are nearly saturated with respect to calcite ($CaCO_3$) and magnesite ($MgCO_3$) in James Creek (Table 7), which is consistent with observations of efflorescent salts on dry sediments. Sources of sulfate to James Creek include oxidation of pyrite in mine workings, tailings, and waste rock along the tributary, the spring at the OHE, and weathering of native soil. The sulfate concentration in James Creek near the confluence with Tributary 1 was elevated for a fresh water [70 to 100 mg/L (0.7 to 1 mM); Table 4], in part due to drainage from Tributary 1, which contained 130 mg/L (1.4 mM).

Fe(III)-(hydr)oxide colloids are common in many tributaries of James Creek and its upper reaches. These colloids are formed by the oxidation of ferrous iron dissolved from iron-sulfide minerals (presumably pyrite) associated with the volcanic sandstone and silica-carbonate alterred serpentinite veins that were mined. Infiltration of water into mined hillsides and the availability of oxygen through open adits promotes pyrite oxidation. Open adits likely yield the highest quantity of colloid-bearing water, but there are also seeps near collapsed adits from which iron-rich water flows, according to our recent observations at the OHE and other mines in the region. Precipitation of Fe(Al,Si)-(hydr)oxides under low-temperature conditions results in small particle size and high specific surface area (i.e., surface area normalized by volume). As a result, these metals may be reactive under organic-rich or anaerobic conditions and should therefore not be considered inert.

Dissolved iron and aluminum concentrations are low in James Creek (<50 to 100 μg/L Fe and 10 to 20 μg/L Al; Table 5), which is consistent with the oxidized and alkaline pH that characterize the portion of James Creek sampled (these conditions usually favor the formation of Al,Fe(III)-(hydr)oxides). Samples containing detectable dissolved iron appear to be supersaturated with respect to iron (hydr)oxides including hematite and goethite, based on thermodynamic calculations (Table 7). This supersaturation suggests that either most of the iron is present as filter-passing (<0.45 μm) colloids—a widely documented occurrence (e.g., Zanker *et al.*, 2003)—or that some unmeasured and unmodeled factors are causing the dissolution of Fe(III), conceivably including organic complexation (Stumm, 1995) and photoreduction (Waite and Morel, 1984). Dissolved silica is relatively abundant in James Creek (20 to 30 mg/L), despite several Si-bearing minerals (clay minerals and potassium-feldspar) being thermodynamically supersaturated (Table 7 and Appendix 1). Metals and metalloids (collectively referred using the shorthand metal(loid)s), including aluminum and silicon, readily coprecipitate with Fe(III). The affect of silica is unclear, although it may partially inhibit the precipitation and reduce the specific surface area of Fe(III)-(hydr)oxides (Doelsch *et al.*, 2001). An unstudied constituent that may be present in colloids is sulfur, which is especially abundant near adits where sulfur in pyrite is oxidized. White-yellow flocs have been observed, sometimes in close association with orange (presumably Fe(III)-rich) flocs but have not yet been characterized. We speculate that

these flocs consist of appreciable amounts of elemental sulfur—formed either by abiotic (dissolved oxygen) or biological (e.g., bacterium *Beggiatoa*) oxidation of sulfide—and hydroxysulfates such as jarosite, which can exist with goethite (FeOOH) (Stoffregen *et al.*, 2000).

On the basis of prior research in controlled laboratory systems and a variety of field-based studies metal-(hydr)oxides sorb metal(loid)s (for reviews, see Brown and Parks, 2001; Brown and Sturchio, 2002), and so we expect that metal(loid)s such as Hg(II), As(V), Cr(VI), and Ni—for which concern has been expressed—are transported as sorption complexes with Fe(III)-(hydr)oxide colloids. With the exception of iron, the differences between dissolved (filtered) and unfiltered metal(loid) concentrations were negligible. The fate of a portion of these metal(loid) contaminants may be affected by the stability of Fe(III)-(hydr)oxide (including its coprecipitates).

Table 4. Temperature, pH, alkalinity, and select anions. All concentration units are mg/L, except ionic strength, which is reported in molar units. Nitrate was not detected (<0.2 mg/L) in any sample.

Sample	Temperature °C	pH	Specific Conduct-ivity (µS/cm)	Alkalinity, mg/L as $CaCO_3$	Anions				
					HCO_3^{-} (1,2)	Cl^-	F^-	SO_4^{2-}	Ionic strength (mol/L)(1)
04JC1	14	8.4	410	114	66	5	0.2	95	0.006
04JC2	16	8.2	450	168	98	5.1	0.2	68	0.007
04JC3	14	8.2	410	118	69	5.1	0.2	94	0.006
04OHE1	19	8.3	210	431		4.5	0.3	130	0.013

Note: (1) Calculated from all available aqueous constituents using a thermodynamic model (section 2.4). (2) Minor fractions of CO_3^{2-} and $H_2CO_3^*$ are also likely present (Appendix 1).

Table 5. Elemental composition of *filtered* (<0.45 µm) water. ICP-MS results. All units are µg/L (microgram per liter) unless otherwise noted. Data highlighted in yellow were used to evaluate saturation indices of selected minerals (Table 7).

Sample	Al	Ba	Ca mg/L	Ce	Co	Cr	Cs	Cu	Eu	Fe	K mg/L	La	Li	Mg mg/L	Mn
04JC1-B	15	33	14	nd	7.6	1.5	0.06	Nd	nd	82	1.8	nd	3.6	44	66
04JC2-B	17	45	36	nd	0.16	1.0	nd	0.56	nd	nd	1.9	0.01	6	35	1.1
04JC3-B	20	32	15	0.01	5.0	1.0	0.05	nd	nd	110	1.8	0.01	3.7	43	45
04OHE1-B	14	140	47	nd	0.09	1.1	0.11	0.73	0.01	nd	2.5	nd	68	110	2.3

Sample	Na mg/L	Nd	Ni	P mg/L	Rb	Sc	SiO_2 mg/L	SO_4 mg/L	Sr	Ti	U	V	Y	Yb	Zn
04JC1-B	5.5		440		5.3	2.7	30	95	140	1	0.11		0.04	0.01	1.8
04JC2-B	7.8	0.02	1.4	0.02	0.59	1.6	17	79	260	0.7	0.71	0.7	0.04		5.2
04JC3-B	5.6	0.02	350		4.9	2.6	27	99	150	1.2	0.14	0.5	0.03		5.3
04OHE1-B	14		1.7		2.8	1.9	17	120	450	1.2	0.48		0.01		3.2

Notes: (1) The following elements were not detected (detection limits in µg/L are in parentheses): Ag (<3), As (<1), Be (<0.05), Bi (<0.2), Cd (<0.02), Dy (<0.005), Er (<0.005), Ga (<0.05), Gd (<0.005), Ge (<0.05), Ho (<0.005), Lu (<0.1), Mo (<2), Nb (<0.2), Pb (<0.05), Pr (<0.01), Sb (<0.3), Se (<1), Sm (<0.01), Ta (<0.02), Tb (<0.005), Th (<0.2), Tl (<0.1), W (0.5), Zr (<0.2).

(2) nd = not detected: Ce (<0.01), Cr (<1), Cs (<0.02), Cu (<0.5), Eu (<0.005), Fe (<50), Ge (<0.05), La (<0.01), Nd (<0.01), P (<0.01), Pb (<0.05), Pr (<0.01), Sm (<0.01), V (<0.5), Yb (<0.005).

Table 6. Elemental composition of *unfiltered* water. ICP-MS results. All units are μg/L (microgram per liter) unless otherwise noted. See Table 5 for detection limits of undetected elements (denoted with an "nd").

Sample	Al	Ba	Ca mg/L	Ce	Co	Cr	Cs	Cu	Dy	Er	Eu	Fe	Gd	Ge	K mg/L	La	Li	Mg mg/L
04JC1	17	34	15	0.08	8.5	2.0	0.06	0.51	0.01	0.01	0.01	1650	0.01	nd	2.0	0.07	3.8	43
04JC2	19	44	37	0.02	0.06	1.1	nd	0.60	Nd	Nd	nd	Nd	0.01	nd	2.0	0.02	6.3	35
04JC3	6.1	34	15	0.05	5.6	1.4	0.05	0.50	0.01	0.01	0.01	1060	0.02	nd	1.9	0.05	4	42
04OHE1	35	140	48	0.09	0.17	nd	0.14	0.94	0.01	0.01	0.01	160	0.01	0.05	2.5	0.04	67	105

Sample	Mn	Na mg/L	Nd	Ni	P mg/L	Pb	Pr	Rb	Sc	SiO_2 mg/L	Sm	SO_4 mg/L	Sr	Ti	U	V	Y	Yb	Zn
04JC1	72	5.3	0.06	480	nd	nd	0.01	5.1	2.7	31	0.02	95	140	1.1	0.12	0.7	0.12	0.01	7.5
04JC2	1.3	7.6	0.02	1.4	0.02	nd	nd	0.56	1.7	17	nd	70	250	0.8	0.73	0.7	0.04	Nd	4.9
04JC3	48	5.3	0.05	380	nd	nd	0.01	4.7	2.6	28	0.01	90	150	1	0.13	0.5	0.1	0.01	6.5
04OHE1	22	13	0.04	1.7	nd	0.08	0.01	2.8	1.9	16	nd	120	450	1.7	0.48	nd	0.05	nd	16

Table 7. Mineral saturation indices (S.I.) under a fixed atmospheric oxygen fugacity of 0.2 (approxmately 10 mg/L dissolved oxygen), based on the Geochemist's Workbench 'thermo.dat' database (http://www.geology.uiuc.edu/Hydrogeology/hydro_thermo.htm).

Mineral name	Chemical formula	Log Q/K[1]			
		JC1	JC2	JC3	OHE
Birnessite	$Na_4Mn_{14}O_{27}{\cdot}9\ H_2O$	62	45	58	48
Todorokite	$(Mn^{2+},Ca,Mg)Mn^{4+}{}_3O_7 \cdot H_2O$	54	39	51	42
Nontronite[2]	$Na_{0.3}Fe^{3+}{}_2(Si,Al)_4O_{10}(OH)_2 \cdot nH_2O$	17.2-18.0	-	17.5-18.2	-
Hematite	Fe_2O_3	12.9		13.2	-
Saponite[2]	$(Mg,Fe)_3(Al,Si)_4\ O_{10}(OH)_2$ $(0.5Ca,Na)_{0.3}$-$4H_2O$	5.7-6.4	3.6-4.2	5.0	5.1-6.5
Goethite	α–FeOOH	6.0	-	6.1	-
Sepiolite	$Mg_4Si_6O_{15}(OH)_2{\cdot}6\ H_2O$	3.5	0.3	1.7	3.2
Illite	$K_{0.65}Al_2Al_{0.65}\ Si_{3.35}O_{10}(OH)_2$	3.4	2.7	3.8	1.8
K-feldspar	$KAlSi_3O_8$	2.5	1.8	2.6	1.3
Kaolinite	$Al_2Si_2O_5(OH)_4$	2.4	2.2	3.0	1.2
Ferrihydrite	$Fe(OH)_3$	1.5	-	1.6	-
Dolomite	$CaMg(CO_3)_2$	1.4	1.7	1.0	2.1
Calcite	$CaCO_3$	-0.1	0.3	-0.3	0.3
Gibbsite	$Al(OH)_3$	-	0.3	0.4	-0.2
Magnesite	$MgCO_3$	-0.2	-0.3	-0.4	0.1
Amorphous	Silica SiO_2	-0.5	-0.7	-0.5	-0.8
Gypsum	$CaSO_4{\cdot}2\ H_2O$	-2.4	-2.2	-2.4	-1.9
Brucite	$Mg(OH)_2$	-3.3	-3.7	-3.7	-2.8
Epsomite	$MgSO_4{\cdot}7\ H_2O$	-4.3	-4.5	-4.3	-3.9

Notes: (1) Q = ion activity product; K = solubility product. Log Q/K > 0 indicates the water was thermodynamically supersaturated with respect to the indicated mineral. However, log Q/K > 0 does not indicate that the mineral was present or would necessarily precipitate (see text).

(2) Several cations, with Na-Nontronite the least supersaturate to Mg-Nontronite most supersaturated.

3.3 Biota

In the following three subsections, two different types of data are discussed: total mercury (Hg_T) in invertebrates, frogs, and fish, and organic mercury in invertebrates, which is presumed to be and hereafter referred to as monomethyl mercury (MMHg). Interpretation of Hg_T in frogs and fish as an indicator of mercury reactivity, biouptake, or trophic transfer is limited, pending MMHg measuremens, by the possibility of these samples having contained cinnabar particles at the time of analysis. To minimize this limitation, the gastrointestinal tracts and external surfaces of all amphibians, where cinnabar most likely resides, were carefully flushed to remove any visible particles. However, extremely fine-grained, invisible, adhesive cinnabar particles and minerals to which inorganic Hg(II) was sorbed likely exist in the amphibians' habitats.

3.3.1 Invertebrates (Hg_T and organic mercury)

The relative contribution to the ecological impairment of James Creek by the OHE relative to other sources of mercury is not clear from invertebrate Hg_T or organic mercury measurements. Hg_T and MMHg was detected in all composite samples of invertebrates (Table 8). The geometric means for MMHg in invertebrates collected from James Creek upstream and downstream of the OHE were not appreciably different (0.057 vs. 0.060 µg/g, with a t-test P = 0.39). MMHg concentrations in 12 samples of invertebrates collected from James Creek upstream of Tributary

1 ranged from 0.03 to 0.1 μg/g, while those in 12 samples collected downstream ranged from 0.03 to 0.3 μg/g. Giant waterbugs collected in Spring and water striders collected in Autumn had the highest MMHg concentrations. Although sample quantity may be insufficient to compare mercury concentrations in invertebrates residing nearer to point sources of mercury with those farther downstream, invertebrate MMHg concentrations collected in Spring from Tributary 1 (approx. 0.1 μg/g) and four samples collected from James Creek at the lower Corona Mine adit drainage (Figs. 1 and 10) in Autumn (0.09 to 0.2 μg/g) were higher than those observed downstream (location JC3).

Average (geometric mean) MMHg concentrations in several invertebrate taxa collected from the James Creek watershed locations, summarized in Table 8 and Figures 15 and 16, were generally higher than those measured at a Bear River watershed 'baseline' station where there are no known point sources of mercury (Alpers *et al.*, 2005). Specifically, dragonflies and water striders contained approximately three times as much MMHg (0.07 *vs.* 0.02 μg/g and 0.09 *vs.* 0.04 μg/g, respectively), dobsonflies were 30 percent higher (0.05 *vs.* 0.04 μg/g), while beetles and predaceous stoneflies contained similar concentrations (0.12 *vs.* 0.11 μg/g and 0.05 μg/g, respectively).

Like other fresh water and marine ecosystems, where mercury in invertebrates has been found to consist of both inorganic and methyl mercury (Berzas Nevado *et al.*, 2003; Faganeli *et al.*, 2003), 40 percent (16 of 39) of predatory insect samples had greater than 50 percent mercury as organic mercury (presumably MMHg; §2.3.3). The mean $MMHg/Hg_T$ proportion was 40 percent ($1\sigma = 30$ percent; Table 8), consisting of the following average proportions per taxon: dragonflies (20 percent), dobsonflies (25 percent), predaceous stoneflies (30 percent), predaceous diving beetles (40 percent), giant waterbugs (50 percent), backswimmers (60 percent), and water striders (80 percent). Compared to a gold mine-impacted ecosystem, the mean $MMHg/Hg_T$ proportion in predatory insects collected from the OHE area was approximately half [cf. 1999–2001 study of Greenhorn Creek, Nevada County, CA, where $MMHg/Hg_T$ averaged 75 percent ($1\sigma = 20$ percent); (Alpers *et al.*, 2005)].

The low proportions of MMHg measured in invertebrates in James Creek and the presence of cinnabar in the creek (Fig. 14) suggest that some invertebrates may have anomolously high mercury concentrations as a result of cinnabar contamination. For example, one dragonfly larva contained 30 μg/g (ww) Hg_T, but only 0.06 μg/g (ww) MMHg, or 0.20 percent. Unlike this and other benthic invertebrates collected, water striders, whose exoskeletons should have been more thoroughly cleaned of particles and which do not feed in sediments, yielded the highest measured $MMHg/Hg_T$ ratios since they likely were least contaminated by cinnabar. The current invertebrate data set is similar to that of a 1998 study by Slotton and Ayers (1999), which showed a similar range of Hg_T concentrations and a subset of anomalously high Hg_T concentrations that are likely due to cinnabar contamination. Other sources of inorganic mercury could be through consumption of phytoplankton and zooplankton, both of which can acquire and excrete dissolved inorganic and methyl mercury from water on relatively short time scales (Pickhardt and Fisher, 2007; Pickhardt *et al.*, 2005; Tsui and Wang, 2004). Therefore, a rigorous assessment of ecological impairment in mercury mine-impacted ecosystems should include methyl mercury measurements in addition to Hg_T, as was performed for invertebrates. The following discussion of invertebrates focuses on methyl mercury concentrations.

Table 8. Mercury and methlymercury in invertebrates collected from James Creek and the Oat Hill Extension Mine. ww = wet weight.

Site	Site Code	Date	Order	Family	Number	Mass (g)	Average Mass (g)	Hg (ug/g) ww	MeHg (ug/g) ww	percent liquid	% MeHg
James Creek upstream of Oat Hill Extension Mine drainage	JC1	5/20/2004	Odonata	Aeshnidae	3	0.92	0.31	0.77	0.063	80	8
			Hemiptera	Gerridae	25	1.66	0.07	0.088	0.088	65	100
			Odonata	Gomphidae	20	2.36	0.12	2.006	0.09	75	5
			Odonata	Gomphidae	20	1.22	0.06	0.499	0.093	77	19
			Plecoptera	Perlidae	10	1.99	0.2	0.155	0.034	77	22
			Plecoptera	Perlidae	20	2.32	0.12	0.064	0.035	80	56
			Odonata	Aeshnidae	1	0.46	0.46	32.1	0.058	78	0
			Hemiptera	Belostomatidae	2	3.19	1.6	0.445	0.277	72	62
			Hemiptera	Gerridae	24	1.59	0.07	0.097	0.096	66	99
			Plecoptera	Perlidae	11	1.35	0.12	1.35	0.061	78	5
Oat Hill Extension wetland area	OHE1	5/20/2004	Odonata	Cordulegastridae	3	1.81	0.6	0.97	0.142	80	15
			Coleoptera	Dytiscidae	30	1.89	0.06	13.5	0.064	51	1
			Hemiptera	Gerridae	25	1.6	0.06	0.20	0.18	69	90
Oat Hill Extension drainage near James Creek	JC2	5/20/2004	Odonata	Cordulegastridae	1	1	1	0.132	0.074	78	57
			Megaloptera	Corydalidae	4	0.9	0.23	0.346	0.064	81	19
			Hemiptera	Gerridae	25	1.79	0.07	0.103	0.079	67	76
			Hemiptera	Gerridae	25	1.5	0.06	0.172	0.127	65	74
Lower Corona Mine-Downstream	CRND	10/29/2004	Hemiptera	Gerridae	8	0.88	0.11	0.173	0.102	77	59
			Hemiptera	Notonectidae	17	1.79	0.11	0.253	0.155	62	61
Lower Corona Mine-Upstream	CRNU		Coleoptera	Dytiscidae	16	0.66	0.04	0.161	0.09	NC[a]	56
			Coleoptera	Dytiscidae	20	0.71	0.04	0.156	0.105	NC	67
James Creek upstream Oat Hill Mine Drain	JC1		Odonata	Aeshnidae	8	1.18	0.15	0.06	0.025	82	41
			Megaloptera	Corydalidae	3	0.93	0.31	0.141	0.042	NC	30
			Hemiptera	Gerridae	25	1.14	0.05	0.135	0.117	53	87
			Odonata	Gomphidae	11	2.5	0.23	0.347	0.042	78	12
			Odonata	Gomphidae	11	2.54	0.23	14.4	0.074	79	1
			Plecoptera	Perlidae	10	1.01	0.1	0.111	0.058	NC	52
James Creek downstream Oat Hill Extension Drain drainage	JC3		Odonata	Aeshnidae	7	1.17	0.17	0.091	0.048	82	53
			Hemiptera	Belostomatidae	2	2.4	1.2	0.128	0.058	80	46
			Hemiptera	Belostomatidae	2	2.66	1.33	0.19	0.069	77	36
			Odonata	Cordulegastridae	1	1.19	1.19	0.216	0.033	85	15
			Hemiptera	Gerridae	25	1.1	0.04	0.086	0.042	71	49
			Hemiptera	Gerridae	25	1.04	0.04	0.097	0.058	68	60
			Odonata	Gomphidae	7	1.6	0.23	0.201	0.051	80	25
			Plecoptera	Perlidae	10	1.01	0.1	0.525	0.065	78	12
Oat Hill Extension wetland area	OHE1		Odonata	Aeshnidae	4	1.07	0.27	4.427	0.09	NC	2
			Odonata	Cordulegastridae	1	0.63	0.63	9.606	0.213	NC	2
			Coleoptera	Dytiscidae	20	1.1	0.06	0.477	0.199	NC	42
			Coleoptera	Dytiscidae	29	1.01	0.03	0.469	0.193	NC	41

MMHg concentrations in invertebrates from the wetland area near OHE (OHE1) suggest that the sediments there produce methyl mercury that is taken up by lower trophic level organisms. Too few samples of invertebrates were collected to statistically compare biouptake of MMHg among sites. Seasonal (Spring *vs.* Autumn) comparisons are also not meaningful, because different taxa were collected in each season. However, MMHg concentrations in certain taxa at certain sites are noteworthy. The most contaminated invertebrates were from the OHE1 location (Table 8 and Figs. 14 and 15), where MMHg concentrations in seven samples of invertebrates ranged from 0.06 to 0.22 μg/g MMHg, five of which exceeded 0.14 μg/g MMHg (Table 8). Of the taxa available at OHE1, dragonflies, water striders, and diving beetles were found to have the highest concentrations of MMHg (all approximately 0.2 μg/g ww, on average) of all the samples collected from the study area. These results demonstrate that MMHg produced in sediments can be taken up by local invertebrates, potentially providing a link between mercury methylation and trophic transfer to higher level organisms.

3.3.2 Frogs (Hg_T)

As is the case for invertebrate data, the ecological impact of the OHE in addition to other sources of mercury to James Creek is not clear from frog Hg_T measurements. Five Foothill Yellow-legged frogs were collected on May 20 and two more on October 29; all were analyzed for Hg_T (Table 9). Average concentrations of Hg_T in frogs from James Creek were similar upstream (0.18 μg/g) and downstream (0.15 μg/g) of OHE drainage and at the lower Corona Mine adit drainage (0.14 μg/g).

Hg_T in foothill yellow-legged frogs collected from the James Creek study area, ranging from 0.1 to 0.6 μg/g Hg (Table 9), was on average twice that of values in an extensive database compiled from studies throughout Northern California[6] (0.2 *vs.* 0.1 μg/g Hg_T), with the highest concentration observed at the wetland area of the OHE in Autumn.

Frogs may be susceptible to trophic transfer of MMHg from invertebrates at this location, on the basis of relatively high Hg_T in one frog (0.6 μg/g, approximately 40 times higher than the ten lowest frog recoveries in the Northern California database) and MMHg in invertebrates at that location. The concentration of Hg_T in this frog from the wetland area of the OHE was exceeded by only 16 of the 190 foothill yellow-legged frogs analyzed by the USGS to-date in Northern CA[7]. While these results suggest that Hg is accumulated in biota above the lowest trophic level in James Creek, further study is required to rule out their misinterpretation due to cinnabar contamination.

3.3.3 Fish (Hg_T)

Like invertebrates and frogs, fish mercury results do not clearly indicate that the OHE site is responsible for ecological impairment of biota in addition to that from other sources of mercury to James Creek. A number of factors could limit the use of fish data for this assessement, including the close proximity of the sampling locations. The fish are more mobile than invertebrates and could have resided upstream and downstream of Tributary 1. Hg_T

[6] Foothill yellow-legged frogs have been collected in various studies in Northern California and analyzed for Hg since 1997. During that period, 190 frogs were analyzed from seven major watersheds, including Cache Creek in the Coast Range, the Bear-Yuba Watershed in the Sierras, the Trinity River, and Upper Clear Creek, including Whiskeytown National Recreation Area (R. Hothem unpubl. data).

[7] These 16 frogs were collected from the Cache Creek or Trinity River watersheds.

Table 9. Mercury concentrations in Foothill Yellow-legged frogs (*Rana boylii*) collected from James Creek and Oat Hill Extension Mine.

Site	Site code	Date	Sample code	Total Mass (g)	Age	Sex	Hg (µg/g dw)	Hg (µg/g ww)	Percent liquid
James Creek upstream Oat Hill Extension (OHE) drainage	JC1	5/20/04	1994	12.4	Adult	Male	0.77	0.18	76.0
James Creek downstream OHE drainage	JC3	5/20/04	1995	28.1	Adult	Female	0.93	0.20	78.0
			1996	20.2	Adult	Female	0.59	0.13	80.2
			1997	15.3	Adult	Male	0.69	0.15	78.2
OHE drainage (Tributary 1)	OHED	5/20/04	1998	3.06	Juvenile	Female	0.84	0.19	77.1
Downstream of lower Corona Mine Adit	CRND	10/29/04	2027	NA	Adult	Female	0.58	0.14	76.5
Oat Hill Extension wetland area	OHE1	10/29/04	2028	NA	Juvenile	Unknown	2.8	0.61	78.2

concentrations in rainbow trout collected from James Creek up- and downstream of Tributary 1 ranged from 0.05 to 0.2 µg/g (geometric mean 0.1 µg/g) and 0.1 to 0.3 µg/g (geometric mean 0.13 µg/g), respectively. It is uncertain whether fillets from rainbow trout collected from James Creek would exceed the U.S. Environmental Protection Agency 2001 advisory level of 0.3 µg of methyl mercury per gram of edible tissue (www.epa.gov/mercury), but whole body Hg_T did not exceed 0.3 µg/g (Table 10; the highest recovery was 0.27 µg/g). California roach upstream and downstream of OHE drainage ranged from 0.1 to 0.2 µg/g Hg_T, (geometric mean 0.16 µg/g). To protect the health of wildlife and humans, a target level of 0.05 µg-*methyl* Hg g^{-1} whole body fish tissue have been set for small (less than four-inch total length) fish such as roach in another California mine-impacted subwatershed of Cache Creek, Harley Gulch (Cooke and Morris, 2005). While the roach collected in this study contain much higher levels of Hg_T, we are not sure what portion is methylated and therefore whether they pose an ecological risk as defined by Cooke and Morris (2005). Beckvar et al. (2005) concluded that 0.2 µg Hg_T g^{-1} whole-body fish tissue (on a wet weight basis) protects the health of juvenile and adult fish, but they did not consider the effect of mercury speciation, a necessary consideration given that the chemical steps required to render cinnabar reactive may be different than those required for different forms of inorganic Hg in other fresh water systems. Whether systems such as James Creek are unique in this regard is unknown. Therefore, broadly databased assessments of mercury toxicity or other bio-relevant behavior that do not explicitly take fundamental inorganic mercury reactivity into account should be applied with caution.

If enough mercury present in James Creek fish is cinnabar, Hg_T concentrations exceeding 0.2 µg/g may still be protective of their health. In addition to water and sediment (section 3.2.1), criteria for Hg_T in predator (0.2 µg/g, presumably after Beckvar et al. (2005)) and prey (0.03 µg/g) fish have been proposed in the Tomales Bay watershed (Marshall, 2006).[8] The effect of

[8] We do not know if Marshall and others were aware of speciation measurements of Kim *et al.* (2004) and Slowey (unpublished data transmitted by letter to Dyan Whyte and J. Marshall, SF Bay RWQCB), finding Hg dominant

mercury speciation in that case was also not explicitly considered. Consequently, it would be dubious to conclude, based on eight percent of fish (3 out of 37) exceeding 0.2 μg/g Hg_T (Table 10), that the aquatic ecology of James Creek is impaired. However, in light of the invertebrate results, the potential for ecological impairment is clearly evident and may manifest in other biota (e.g., piscivorous birds).

California roach had significantly higher Hg_T on average than trout (0.16 μg/g for 14 roach samples vs. 0.12 μg/g for 23 trout samples; test done with logged data), based on a *P* value of 0.03 for a one-tailed *t* test assuming equal variance for roach and trout Hg_T. Compared with the same species from other sites in Northern California, fish from James Creek were moderately contaminated with Hg[9]. Similar fish Hg_T was measured in Spring 1998 in small and juvenile fish above the confluence of Tributary 1 with James Creek (Slotton and Ayers, 1999).

Fish Hg_T concentrations *in muscle tissue* (on a wet weight basis) have been found to positively and non-linearly correlate to body length in other mine-impacted settings by Slotton et al. (2004), who were cognizant, unlike others (Jewett *et al*., 2003), of the potential for wide-ranging Hg concentrations to falsely imply this correlation. To linearize the relationship and normalize the errors as required in tests of significance, we $\log_{10}$ transformed our fish Hg_T (ppm wet weight) and length (mm) data prior to exploring their possible correlation. Because rainbow trout and California roach have different eating habits (trout are primarily insectivores, feeding on insects in drift and on the water surface, while roach are omnivores, eating algae and insects at or near sediment), we investigated each fish species data set separately. For the case of *whole-body* Hg_T analyses of James Creek trout and roach collected during this study, $\log_{10}$ fish Hg_T is correlated to total length (Fig. 17). However, the significance of these correlations is a matter of interpretation. Analysis of variance (ANOVA), which compares the variance of the $\log_{10}$ Hg_T data with the variance about the best-fit function, suggests that, 3.7 percent of the time, a correlation this large ($R^2 = 0.19$) could happen by chance alone. ANOVA of roach data suggest the observed correlation ($R^2 = 0.46$) could happen 9.4 percent of the time by chance alone. The likelihoods of improving estimation is the most interpretive part of these correlation results, and would depend on the policy implications and/or remedial expenditures. Given that the correlations are at best marginally significant with this small number of samples, validation of this putative correlation would require additional fish sampling.

For a single fish species, or among species of similar lifestyle and physiology, the presence or absence of a significant correlation between Hg and length is likely related, among other factors, to the proportion of MMHg to total Hg. Since MMHg is retained more than inorganic Hg, a stronger correlation with length will likely characterize fish containing higher proportions of MMHg. In the present study, we have no direct evidence of this proportion at this time. We would like to conclude whether the majority of Hg in the fish collected is methylated or not, because this distinction is critical to knowning whether the mercury in James Creek taken up by biota will likely be retained long enough to impact the ecology of the larger Putah Creek

---

cinnabar and metacinnabar in the source mine waste and apparent colloid transport of mercury to Gambonini Creek due to organic acids in hydrophytic plants, the processes of which was studied by Slowey *et al*. (2005a).

[9] Compared with 62 samples of California roach collected from Northern California since 1999 (R. Hothem, unpubl. data), which had a geometric mean of 0.14 μg/g Hg, the James Creek roach had a mean concentration of 0.16 μg/g. A total of 406 samples of rainbow trout collected from Northern California since 1999 (R. Hothem, unpubl. data) had a geometric mean of 0.115 μg/g Hg, compared with 0.122 μg/g from James Creek.

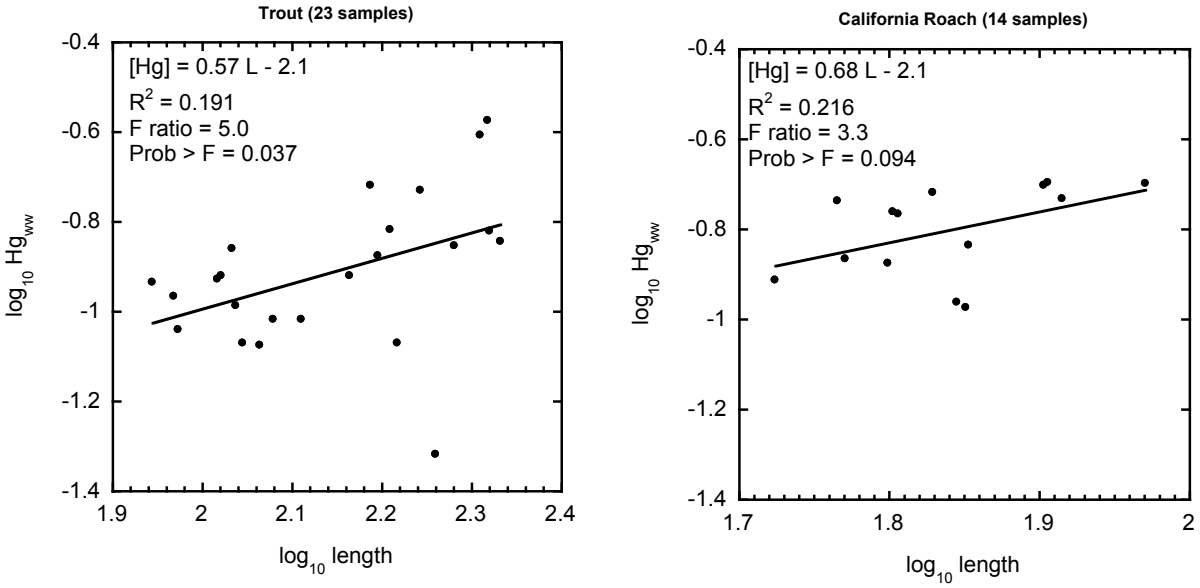

Figure 17. Log_{10} transforms of Hg_T (ppm, wet-weight basis) in Rainbow Trout and California Roach ([Hg]) compared to log_{10} transforms of total fish body length in mm (L). See text for an explanation as to why the data were log-transformed. The results of the regression analysis includes the squared correlation coefficient R^2 which denotes the proportion of variance of Hg accounted for by length and analysis of variance (ANOVA) significance tests in which the *F ratio* statistic evaluates the probability that a relationship this strong could be made by chance, as is more fully explained in the text.

watershed, including Lake Berryessa. Given the policy implications of interpreting these and other biota data, we strongly discourage reliance on other studies (e.g., Bloom, 1992) as the basis for interpreting total mercury measurements as indicative of methyl mercury uptake. Appreciably different conditions at locations such as James Creek compared to systems that are more extensively studied (e.g., those receiving mercury primarily as a result of atmospheric deposition, not past mining) may have decisive implications.

To our knowledge, study of the proportion of methyl to total mercury in fish residing in cinnabar mine-impacted riverine systems is limited to two studies of the Yukon-Kuskokwim delta, Alaska (Gray *et al*., 2000; Jewett *et al*., 2003). Gray *et al*. (2000) sampled Arctic grayling (a low trophic-level fish) from Cinnabar Creek, a tributary of the Kuskokwim River known to contain cinnabar. The muscle tissue of three of these grayling were analyzed for both Hg_T and MMHg, finding 94 to 127 percent of mercury was methylated. Allowing for analytical errors evident from these results suggeststst that most if not all mercury in *muscle tissue* of these fish species is methylated. In discussing these and the James Creek results, Gray noted there is a legitimate concern that an appreciable portion of mercury measured in *whole-body* samples of fish from a cinnabar-contaminated creek could be inorganic (*pers. comm.* March 28, 2007). At other locations along the Yukon and Kuskokwim Rivers, Jewett *et al*. (2003) found that, on average, 94 percent of mercury in pike muscle was methylated, but these fish were not collected near tributaries known to contain cinnabar (mercury in water or sediment was not measured). In conclusion, there currently is no strong basis on which to assume that the mercury measured in whole-body fish samples is mostly methylated. We recommend that, given the cost of MMHg

analysis, a subset of fish samples be analyzed for both Hg_T and MMHg and, when possible, to analyze muscle tissue in lieu of whole bodies.

3.3.4 Trophic transfer of mercury

On a sample-averaged basis at the two James Creek locations JC1 and JC3, frogs, roach, and trout all had higher levels of mercury than invertebrates (Fig. 18). Invertebrate MMHg was compared with upper trophic level biota to avoid bias due to the apparent ingestion by or adhesion of cinnabar to invertebrates. Estimation of bioaccumulation factors (BAFs) would be better supported by consistent use of MMHg data, since Hg_T in these frogs and fish may include inorganic mercury resulting in overestimation of BAFs.

4. Conclusions

The OHE tailings are unusual in comparison to most mercury mine tailings because they were not heated in a retort or furnace. Processing of the ores through a gravity circuit to recover cinnabar concentrates resulted in tailings that should have considerably higher residual cinnabar and metal-sulfide mineals such as pyrite. The tailings, containing 600 to 1,000 ppm mercury, contaminate a tributary (*Tributary 1*) that drains the OHE area into James Creek. The 1,500 ppm mercury recovered from sediment in a drainage that transects the tailings pile (Drainage A) suggests that mercury-enriched sediment will be transported from the tailings during both base and high flows. However, there are other sources of mercury, including mercury-enriched (930 to 1,200 ppm) tailings above the OHE mine area from a dump near the USBLM property boundary (presumably from a past Oat Hill mining operation). Water from a spring located below the adit at the OHE had high Hg_T (780 ng/L), elevated sulfate (130 mg/L), and is saturated with respect to calcite and magnesite, both of which were observed in the spring sediment. This spring water flows into Tributary 1, which then flows into James Creek. Elevated concentration of mercury and sulfate in James Creek below the confluence with Tributary 1 may, therefore, partly result from drainage from this spring (Drainage B). Dispersion along this hydrological pathway is suggested by Hg and sulfate results (listed from Drainage B to Tributary 1 to James Creek): 780 to 14 to 7 ng/L Hg_T; similarly, 130 to 70 to 90 mg/L sulfate.

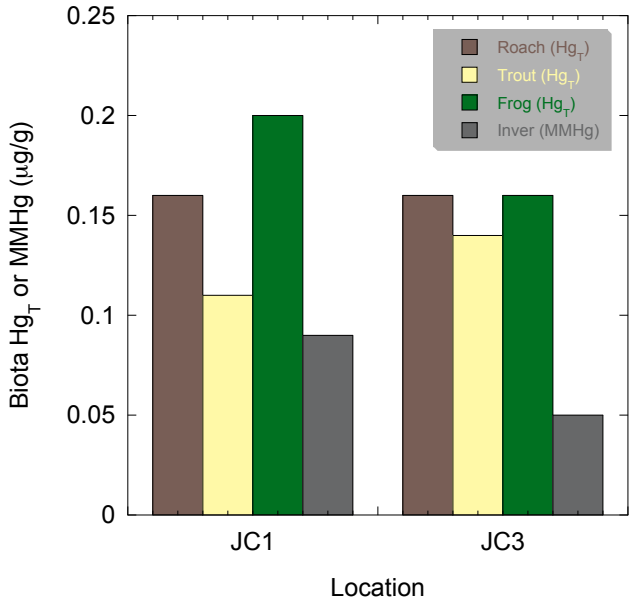

Figure 18. Average concentrations of MMHg in invertebrates and Hg_T in Foothill Yellow-legged frogs, California Roach, and Rainbow Trout sampled from James Creek locations JC1 and JC3 (Fig. 1).

Table 10. Mercury concentrations in fish collected from James Creek on May 20, 2004.

Site	Site Code	Unique Sample Code	Common Name	Number	Total Length (ave. mm)	Hg (ug/g dw)	Hg (ug/g ww)	percent Moisture
James Creek upstream Oat Hill Extension drainage (Tributary 1)	JC1	CR-JC1-001F	California roach	4	93.5	0.890	0.200	77.5
		CR-JC1-002F	California roach	4	82.3	0.828	0.185	77.6
		CR-JC1-003F	California roach	1	80.0	0.891	0.198	77.8
		CR-JC1-004F	California roach	4	71.3	0.669	0.146	78.2
		CR-JC1-005F	California roach	1	70.0	0.496	0.109	78.1
		CR-JC1-006F	California roach	4	63.5	0.759	0.173	77.2
		CR-JC1-007F	California roach	1	53.0	0.538	0.122	77.3
		CR-JC1-015F	Rainbow trout	1	215.0	0.469	0.143	69.5
		CR-JC1-016F	Rainbow trout	1	191.0	0.483	0.140	71.0
		CR-JC1-017F	Rainbow trout	1	182.0	0.152	0.048	68.7
		CR-JC1-018F	Rainbow trout	1	175.0	0.849	0.186	78.1
		CR-JC1-019F	Rainbow trout	1	157.0	0.524	0.133	74.6
		CR-JC1-020F	Rainbow trout	1	111.0	0.376	0.085	77.3
		CR-JC1-021F	Rainbow trout	1	109.0	0.462	0.103	77.7
		CR-JC1-022F	Rainbow trout	1	108.0	0.610	0.138	77.4
		CR-JC1-023F	Rainbow trout	1	104.0	0.513	0.118	77.0
		CR-JC1-024F	Rainbow trout	1	94.0	0.423	0.091	78.5
James Creek downstream Oat Hill Extension drainage (Tributary 1)	JC3	CR-JC3-008F	California roach	4	80.5	0.869	0.201	76.9
		CR-JC3-009F	California roach	4	67.5	0.815	0.191	76.6
		CR-JC3-010F	California roach	1	71.0	0.455	0.106	76.6
		CR-JC3-011F	California roach	4	63.0	0.538	0.133	75.2
		CR-JC3-012F	California roach	1	64.0	0.845	0.171	79.8
		CR-JC3-013F	California roach	4	58.3	0.756	0.183	75.8
		CR-JC3-014F	California roach	1	59.0	0.548	0.136	75.1
		CR-JC3-025F	Rainbow trout	1	209.0	0.476	0.151	68.2
		CR-JC3-026F	Rainbow trout	1	208.0	1.140	0.266	76.7
		CR-JC3-027F	Rainbow trout	1	204.0	1.160	0.247	78.7
		CR-JC3-028F	Rainbow trout	1	165.0	0.302	0.085	71.7
		CR-JC3-029F	Rainbow trout	1	162.0	0.675	0.152	77.5
		CR-JC3-030F	Rainbow trout	1	154.0	0.855	0.191	77.7
		CR-JC3-031F	Rainbow trout	1	146.0	0.507	0.120	76.4
		CR-JC3-032F	Rainbow trout	1	129.0	0.397	0.096	75.8
		CR-JC3-033F	Rainbow trout	1	120.0	0.380	0.096	74.8
		CR-JC3-034F	Rainbow trout	1	116.0	0.346	0.084	75.7
		CR-JC3-035F	Rainbow trout	1	105.0	0.505	0.120	76.2
		CR-JC3-036F	Rainbow trout	1	93.0	0.449	0.108	75.9
		CR-JC3-037F	Rainbow trout	1	88.0	0.512	0.116	77.3

Placer cinnabar has historically been mined from James Creek, and seasonal enrichment of the cinnabar in James Creek has been reported in at least one report (Yates and Hilpert, 1946), presumably due to erosion of mercury-enriched sediment from the Oat Hill and OHE mines during winter storm events. Panned concentrates containing appreciable amounts of cinnabar were obtained from James Creek both above and below the confluence with Tributary 1, indicating that significant sources of mercury-enriched sediment are released from both the Oat Hill[10] and OHE mine sites. A larger amount of cinnabar was apparent in the panned concentrate above Tributary 1, tentatively suggesting that the Oat Hill Mine site may be a more significant source of cinnabar than the OHE Mine to the nearest reach of James Creek (other mine sites may have more or less impact on James Creek as a whole).

High levels of mercury present in sediment and water at the OHE spring, Tributary 1, and James Creek did not result in correspondingly high concentrations of MMHg in the apparently aerobic water and sediment sampled. This finding is likely due to the stability of cinnabar in water and sediments containing low concentrations of organic matter and sulfide and/or degradation of MMHg. To better evaluate the methylation potential of the James Creek system and enhancement of this potential by nearby mine sites, additional sampling and analysis of sediments where MMHg production is more likely to occur should be performed. These locations include root-stabilized fluvial and riparian sediments and wetlands. Although localized production of MMHg may not yield appreciable MMHg concentrations in the bulk waters of James Creek, accumulation of MMHg in fish in mine-impacted waters can be facilitated by uptake of MMHg by benthic invertebrates followed by their consumption by bottom-feeding fish (Slotton *et al*., 2004).

While there is evidence from measurements of water, sediment, and biota that mercury from the OHE and other mines may be impairing the James Creek ecosystem, the measurements suggest that the degree of impairment is not commensurate with the extraordinary degree of mercury contamination present. Methyl mercury concentrations in flowing water and sediment from James Creek and the tributary that drains the OHE are relatively low, ranging from 0.04 to 0.08 ng/L, although these data should be interpreted with caution (see § 3.2).

While the results of this investigation suggest that the OHE contributes inorganic mercury to James Creek, they do not indicate whether the OHE site is ecologically impairing biota in addition to impairment from other sources of mercury to James Creek, nor do they provide any indication of the relative importance of the OHE to the ecological impairment.

Acknowledgments. This field investigation was funded by the USBLM, who also granted access to study locations. We thank David Lawler (USBLM) for sampling assistance. Permission to collect biological specimens for study was kindly granted by the California Department of Fish and Game. Ion chromatography and alkalinity analyses were performed by USGS laboratories under the direction of Paul Lamothe. ICP-AES analyses were performed in USGS laboratories under the direction of Paul Briggs. R. Taylor of TERL and C. Davies of Brooks Rand conducted or oversaw the chemical analyses of biota. K. DeClercq and A. Meckstroth helped collect biota.

[10] See footnote 1, p. 2.

Forthright and careful reviews by Roger Ashley and Steve Ludington (USGS) improved this report. AJS gratefully acknowledges the help of Donald Singer (USGS) with statistics.

5. References

Alpers, C. N., Hunerlach, M. P., May, J. T., Hothem, R. L., Taylor, H. E., Antweiler, R. C., DeWild, J. F., Lawler, D. A., 2005. Geochemical characterization of water, sediment, and biota affected by mercury contamination and acidic drainage from historical gold mining, Greenhorn Creek, Nevada County, California, 1999-2001. *U.S. Geological Survey Scientific Investigations Report*. **2004-525**, 278 pp.

Banfield, J. F., Welch, S. A., Zhang, H. Z., Ebert, T. T., Penn, R. L., 2000. Aggregation-based crystal growth and microstructure development in natural iron oxyhydroxide biomineralization products. *Science* **289**, 751-754.

Barrow, N. J., Cox, V. C., 1992. The Effects of pH and chloride concentration on mercury sorption 1. By goethite. *J. Soil Sci.* **43**, 295-304.

Benoit, J. M., Gilmour, C. C., Heyes, A., Mason, R. P., Miller, C. L., 2003. Geochemical and biological controls over methylmercury production and degradation in aquatic ecosystems. In: Cai, Y., Braids, O. C. (Eds.), *Biogeochemistry of Environmentally Important Trace Elements*. **835 ACS Symposium Series** Oxford University Press, Oxford. pp. 262-297.

Benoit, J. M., Gilmour, C. C., Mason, R. P., 2001. The influence of sulfide on solid-phase mercury bioavailability for methylation by pure cultures of *Desulfobulbus propionicus* (1pr3). *Environ. Sci. Technol.* **35**, 127-132.

Berzas Nevado, J. J., Garcia Bermejo, L. F., Rodriguez Martin-Doimeadios, R. C., 2003. Distribution of mercury in the aquatic environment at Almaden, Spain. *Environ. Pollut.* **122**, 261-271.

Bloom, N. S., 1992. On the Chemical Form of Mercury in Edible Fish and Marine Invertebrate Tissue. *Can. J. Fish. Aquat. Sci.* **49**, 1010-1017.

Bloom, N. S., 1995. Mercury as a case study of ultra-clean sample handling and storage in aquatic trace metal research. *Environmental Laboratory* **3-4**, 20-25.

Bloom, N. S., 2001. Solid Phase Hg Speciation and Incubation Studies in or Related to Mine-site Runoff in the Cache Creek Watershed (CA). *Assessment of Ecological and Human Health Impacts of Mercury in the San Francisco Bay-Delta Watershed*. 37 pp. California Bay Delta Authority, Sacramento.

Bloom, N. S., Crecelius, E. A., Fitzgerald, W. F., 1988. Determination of volatile mercury species at the picogram level by low temperature gas chromatography with cold vapor atomic fluorescence detection. *Anal. Chim. Acta* **208**, 151-161.

Brown, G. E., Jr., Parks, G. A., 2001. Sorption of trace elements on mineral surfaces: Modern perspectives from spectroscopic studies, and comments on sorption in the marine environment. *Int. Geol. Rev.* **43**, 963-1073.

Brown, G. E., Sturchio, N. C., 2002. An overview of synchrotron radiation applications to low temperature geochemistry and environmental science. In: Fenter, P. A., Rivers, M. L., Sturchio, N. C., Sutton, S. R. (Eds.), *Applications of Synchrotron Radiation in Low-Temperature Geochemistry and Environmental Sciences. Rev. Mineral. Geochem.* **49** Mineralogical Society of America, Washington, DC. pp. 1-115.

Conaway, C. H., Watson, E. B., Flanders, J., Flegal, A. R., 2004. Mercury deposition in a tidal marsh of south San Francisco Bay downstream of the historic New Almaden mining district, California. *Mar. Chem.* **90**, 175-184.

Crock, J. G., 1996. Mercury. In: Sparks, D. L. (Ed.), *Methods of Soil Analysis, Part 3. Chemical Methods*. **5** Soil Science Society of America, Madison, WI. pp. 769-791.

Doelsch, E., Stone, W. E. E., Petit, S., Masion, A., Rose, J., Bottero, J. Y., Nahon, D., 2001. Speciation and crystal chemistry of Fe(III) chloride hydrolyzed in the presence of SiO4 ligands. 2. Characterization of Si-Fe aggregates by FTIR and Si-29 solid-state NMR. *Langmuir* **17**, 1399-1405.

Ericksen, J. A., Gustin, M. S., Lindberg, S. E., Olund, S. D., Krabbenhoft, D. P., 2005. Assessing the potential for re-emission of mercury deposited in precipitation from arid soils using a stable isotope. *Environ. Sci. Technol.* **39**, 8001-8007.

Faganeli, J., Horvat, M., Covelli, S., Fajon, V., Logar, M., Lipej, L., Cermelj, B., 2003. Mercury and methylmercury in the Gulf of Trieste (northern Adriatic Sea). *Sci. Total Environ.* **304**, 315-326.

Fishman, M. J., Friedman, L. C., 1989. Ion Chromatography, *Methods for Determination of Inorganic Substances in Water and Fluvial Sediments. Techniques of Water-Resources Investigations of the United States Geological Survey*. U.S. Geological Survey, http://pubs.usgs.gov/twri/twri5-a1/pdf/twri_5-A1_b.pdf. pp. 38-43.

Fleming, E. J., Mack, E. E., Green, P. G., Nelson, D. C., 2006. Mercury methylation from unexpected sources: Molybdate-inhibited freshwater sediments and an iron-reducing bacterium. *Appl. Environ. Microbiol.* **72**, 457-464.

Gilbert, B., Banfield, J. F., 2005. Molecular-scale processes involving nanoparticulate minerals in biogeochemical systems. In: Banfield, J., CerviniSilva, J., Nealson, K. (Eds.), *Molecular Geomicrobiology. Reviews in Mineralogy & Geochemistry*. **59** Mineralogical Society of America and Geochemical Society, Virginia. pp. 109-155.

Gilmour, C. C., Henry, E. A., Mitchell, R., 1992. Sulfate stimulation of mercury methylation in freshwater sediments. *Environ. Sci. Technol.* **26**, 2281-2287.

Gray, J., Theodorakos, P., Bailey, E., Turner, R., 2000. Distribution, speciation, and transport of mercury in stream-sediment, stream-water, and fish collected near abandoned mercury mines in southwestern Alaska, USA. *Sci. Total Environ.* **260**, 21-33.

Gustin, M. S., Coolbaugh, M. F., Engle, M. A., Fitzgerald, B. C., Keislar, R. E., Lindberg, S. E., Nacht, D. M., Quashnick, J., Rytuba, J. J., Sladek, C., Zhang, H., Zehner, R. E., 2003. Atmospheric mercury emissions from mine wastes and surrounding geologically enriched terrains. *Environ. Geol.* **43**, 339-351.

Gustin, M. S., Ericksen, J. A., Schorran, D. E., Johnson, D. W., Lindberg, S. E., Coleman, J. S., 2004. Application of controlled mesocosms for understanding mercury air-soil-plant exchange. *Environ. Sci. Technol.* **38**, 6044-6050.

Helgeson, H. C., 1969. Thermodynamics of Hydrothermal Systems at Elevated Temperatures and Pressures. *Am. J. Sci.* **267**, 729-804.

Horvat, M., Bloom, N. S., Liang, L., 1993a. A comparison of distillation with other current isolation methods for the determination of methyl mercury compounds in low level environmental samples, part 2, water. *Anal. Chim. Acta* **282**, 153-168.

Horvat, M., Bloom, N. S., Liang, L., 1993b. Comparison of distillation with other current isolation methods for the determination of methyl mercury compounds in low level environmental samples: Part 1. Sediments. *Anal. Chim. Acta* **281**, 135-152.

Jay, J. A., Morel, F. M. M., Hemond, H. F., 2000. Mercury speciation in the presence of polysulfides. *Environ. Sci. Technol.* **34**, 2196-2200.

Jay, J. A., Murray, K. J., Gilmour, C. C., Mason, R. P., Morel, F. M. M., Roberts, A. L., Hemond, H. F., 2002. Mercury methylation by *Desulfovibrio desulfuricans* ND132 in the presence of polysulfides. *Appl. Environ. Microbiol.* **68**, 5741-5745.

Jewett, S. C., Zhang, X. M., Naidu, A. S., Kelley, J. J., Dasher, D., Duffy, L. K., 2003. Comparison of mercury and methylmercury in northern pike and Arctic grayling from western Alaska rivers. *Chemosphere* **50**, 383-392.

Kappler, A., Straub, K. L., 2005. Geomicrobiological Cycling of Iron. In: Banfield, J. F., Cervini-Silva, J., Nealson, K. H. (Eds.), *Molecular Geomicrobiology. Rev. Mineral. Geochem.* **59** Mineralogical Society of American and Geochemical Society, Virginia. pp. 85-108.

Kerin, E. J., Gilmour, C. C., Roden, E., Suzuki, M. T., Coates, J. D., Mason, R. P., 2007. Mercury methylation by dissimilatory iron-reducing bacteria. *Appl. Environ. Microbiol.* **72**, 7919-7921.

Kim, C. S., Rytuba, J. J., Brown, G. E., Jr., 2004. Geological and anthropogenic factors influencing mercury speciation in mine wastes: an EXAFS spectroscopy study. *Appl. Geochem.* **19**, 379-393.

Lowry, G. V., Shaw, S., Kim, C. S., Rytuba, J. J., Brown, G. E., Jr., 2004. Particle-facilitated mercury transport from New Idria and Sulphur Bank mercury mine tailings: Column experiments and macroscopic, microscopic and spectroscopic analysis. *Environ. Sci. Technol.* **38**, 5101-5111.

Merritt, K. A., Amirbahman, A., 2007. Mercury Mobilization in Estuarine Sediment Porewaters: A Diffusive Gel Time-Series Study. *Environ. Sci. Technol.* **41**, 717-722.

Nordstrom, D. K., Southam, G., 1997. Geomicrobiology of sulfide mineral oxidation. In: Banfield, J. F., Nealson, K. H. (Eds.), *Geomicrobiology: Interactions between Microbes and Minerals. Rev. Mineral. Geochem.* **35** Mineralogical Society of America, Washington, D.C. pp. 361-390.

O'Leary, R. M., Hageman, P. L., Crock, J. G., 1996. Determination of mercury in water, geologic, and plant materials by continuous flow-cold vapor-atomic absorption spectrophotometry. In: Arbogast, B. F. (Ed.), *Analytical methods for the Mineral Resource Surveys Program.* **Open File Report 96-525** U.S. Geological Survey, Denver. pp. 42-55.

Paquette, K. E., Helz, G. R., 1997. Inorganic speciation of mercury in sulfidic waters: The importance of zero-valent sulfur. *Environ. Sci. Technol.* **31**, 2148-2153.

Parker, J. L., Bloom, N. S., 2005. Preservation and storage techniques for low-level aqueous mercury speciation. *Sci. Total Environ.* **337**, 253-263.

Pickhardt, P. C., Fisher, N. S., 2007. Accumulation of inorganic and methylmercury by freshwater phytoplankton in two contrasting water bodies. *Environ. Sci. Technol.* **41**, 125-131.

Pickhardt, P. C., Folt, C. L., Chen, C. Y., Klaue, B., Blum, J. D., 2005. Impacts of zooplankton composition and algal enrichment on the accumulation of mercury in an experimental freshwater food web. *Sci. Total Environ.* **339**, 89-101.

Poulton, S. W., Krom, M., Raiswell, R., 2004. A revised scheme for the reactivity of iron (oxyhydr)oxide minerals towards dissolved sulfide. *Geochim. Cosmochim. Acta* **68**, 3703-3715.

Pyzik, A., Sommer, S., 1981. Sedimentary iron monosulfides: kinetics and mechanism of formation. *Geochim. Cosmochim. Acta* **45**, 687-698.

Rickard, D., Morse, J. W., 2005. Acid volatile sulfide (AVS). *Mar. Chem.* **97**, 141-197.

Rounds, S. A., 2006. Alkalinity and acid neutralizing capacity. In: Wilde, F. D. (Ed.), *National field manual for the collection of water-quality data: U.S. Geological Survey Techniques of Water-Resources Investigations.* U.S. Geological Survey. http://pubs.water.usgs.gov/twri9A.

Seeberg-Elverfeldt, J., Schluter, M., Feseker, T., Kolling, M., 2005. Rhizon sampling of porewaters near the sediment-water interface of aquatic systems. *Limnol. Oceanogr. Methods* **3**, 361-371.

Sellers, P., Kelly, C. A., Rudd, J. W. M., MacHutchon, A. R., 1996. Photodegradation of methylmercury in lakes. *Nature* **380**, 694-697.

Sigg, L., Black, F., Buffle, J., Cao, J., Cleven, R., Davison, W., Galceran, J., Gunkel, P., Kalis, E., Kistler, D., Martin, M., Noel, S., Nur, Y., Odzak, N., Puy, J., vanRiemsdijk, W., Temminghoff, E., Tercier-Waeber, M. L., Toepperwien, S., Town, R. M., Unsworth, E., Warnken, K. W., Weng, L., Xue, H., Zhang, H., 2006. Comparison of analytical techniques for dynamic trace metal speciation in natural freshwaters. *Environ. Sci. Technol.* **40**, 1934-1941.

Slotton, D. G., Ayers, S. M., 1999. Pope Creek Watershed 1998 Biological Mercury Assessment. 45 pp. for Public Resource Associates, San Francisco, CA and Reno, NV.

Slotton, D. G., Ayers, S. M., Suchanek, T. H., Weyand, R. D., Liston, A. M., 2004. Mercury Bioaccumulation and Trophic Transfer in the Cache Creek Watershed of California in Relation to Diverse Aqueous Mercury Exposure Conditions. *Assessment of Ecological and Human Health Impacts of Mercury in the San Francisco Bay-Delta Watershed.* 74 pp. California Bay Delta Authority, Sacramento.

Slowey, A. J., Brown Jr., G. E., 2007. Transformations of mercury, iron, and sulfur during the reductive dissolution of iron oxyhydroxide by sulfide. *Geochim. Cosmochim. Acta* **71**, 877-894.

Slowey, A. J., Johnson, S. B., Rytuba, J. J., Brown, G. E., Jr., 2005a. Role of organic acids in promoting colloid transport of mercury from mine tailings. *Environ. Sci. Technol.* **39**, 7869-7874.

Slowey, A. J., Rytuba, J. J., Brown, G. E., Jr., 2005b. Speciation of mercury and mode of transport from placer gold mine tailings. *Environ. Sci. Technol.* **39**, 1547-1554.

Stoffregen, R. E., Alpers, C. N., Jambor, J. L., 2000. Alunite-jarosite crystallography, thermodynamics, and geochronology. In: Alpers, C. N., Jambor, J. L., Nordstrom, D. K. (Eds.), *Sulfate Minerals: Crystallography, Geochemistry and Environmental Significance. Rev. Mineral. Geochem.* **40** Mineralogical Society of America, Washington D.C. pp. 453-479.

Stumm, W., 1995. The Inner-Sphere Surface Complex-A Key to Understanding Surface Reactivity, *Aquatic Chemistry. Advances in Chemistry Series.* **244** American Chemical Society, Columbus, OH. pp. 1-32.

Tsui, M. T. K., Wang, W.-X., 2004. Uptake and elimination routes of inorganic mercury and methylmercury in *Daphnia magna. Environ. Sci. Technol.* **38**, 808-816.

United States Bureau of Mines, 1965. *Mercury potential of the United States.* Information Circular 8252.

United States Environmental Protection Agency, 2002. Method 1631, Revision E: Mercury in Water by Oxidation, Purge and Trap, and Cold Vapor Atomic Fluorescence Spectrometry. *Report 821-R-02-019*, http://www.epa.gov/waterscience/methods/1631e.pdf.

Uthe, J. F., Solomon, J., Grift, B., 1972. Rapid semimicro method for the determination of methylmercury in fish tissue. *J. Assoc. Official Anal. Chem.* **55**, 583-589.

Waite, T. D., Morel, F. M. M., 1984. Photoreductive dissolution of colloidal iron oxide: Effect of citrate. *J. Colloid Interf. Sci.* **102**, 121-137.

Waples, J., Nagy, K. L., Aiken, G. R., Ryan, J. N., 2005. Dissolution of cinnabar (HgS) in the presence of natural organic matter. *Geochim. Cosmochim. Acta* **69**, 1575-1588.

Whyte, D. C., Kirchner, J. W., 2000. Assessing water quality impacts and cleanup effectiveness in streams dominated by episodic mercury discharges. *Sci. Total Environ.* **260**, 1-9.

Yates, R. G., Hilpert, L. S., 1946. Quicksilver deposits of the Eastern Mayacmas District, Lake and Napa Counties, California. *California Journal of Mines and Geology Report XLII of the State Mineralogist*, 231-286.

Zanker, H., Richter, W., Huttig, G., 2003. Scavenging and immobilization of trace contaminants by colloids in the waters of abandoned ore mines. *Colloids Surfaces A: Physicochem. Eng. Aspects* **217**, 21-31.

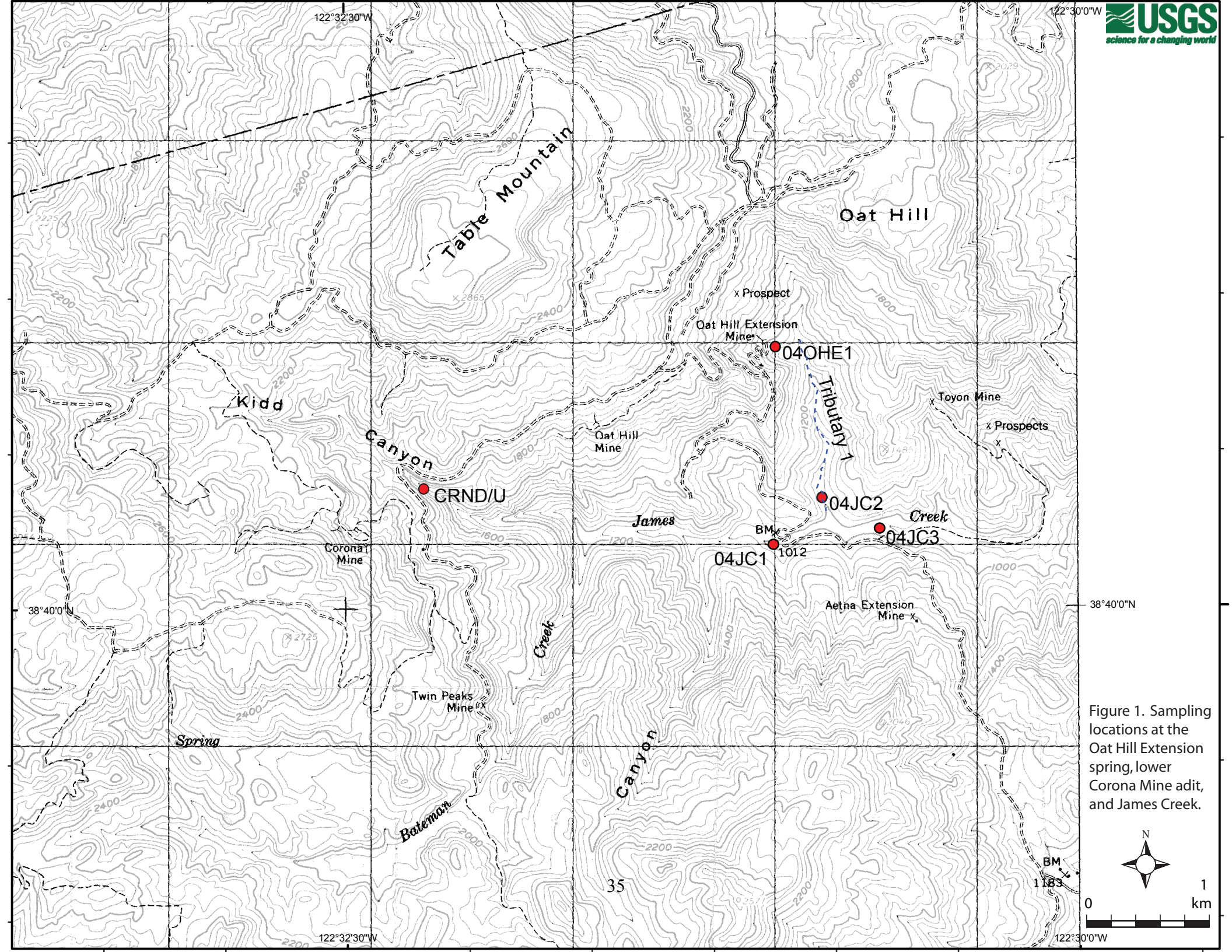

Figure 1. Sampling locations at the Oat Hill Extension spring, lower Corona Mine adit, and James Creek.

Figure 2. Tailings and sediment sampling locations.

USGS science for a changing world

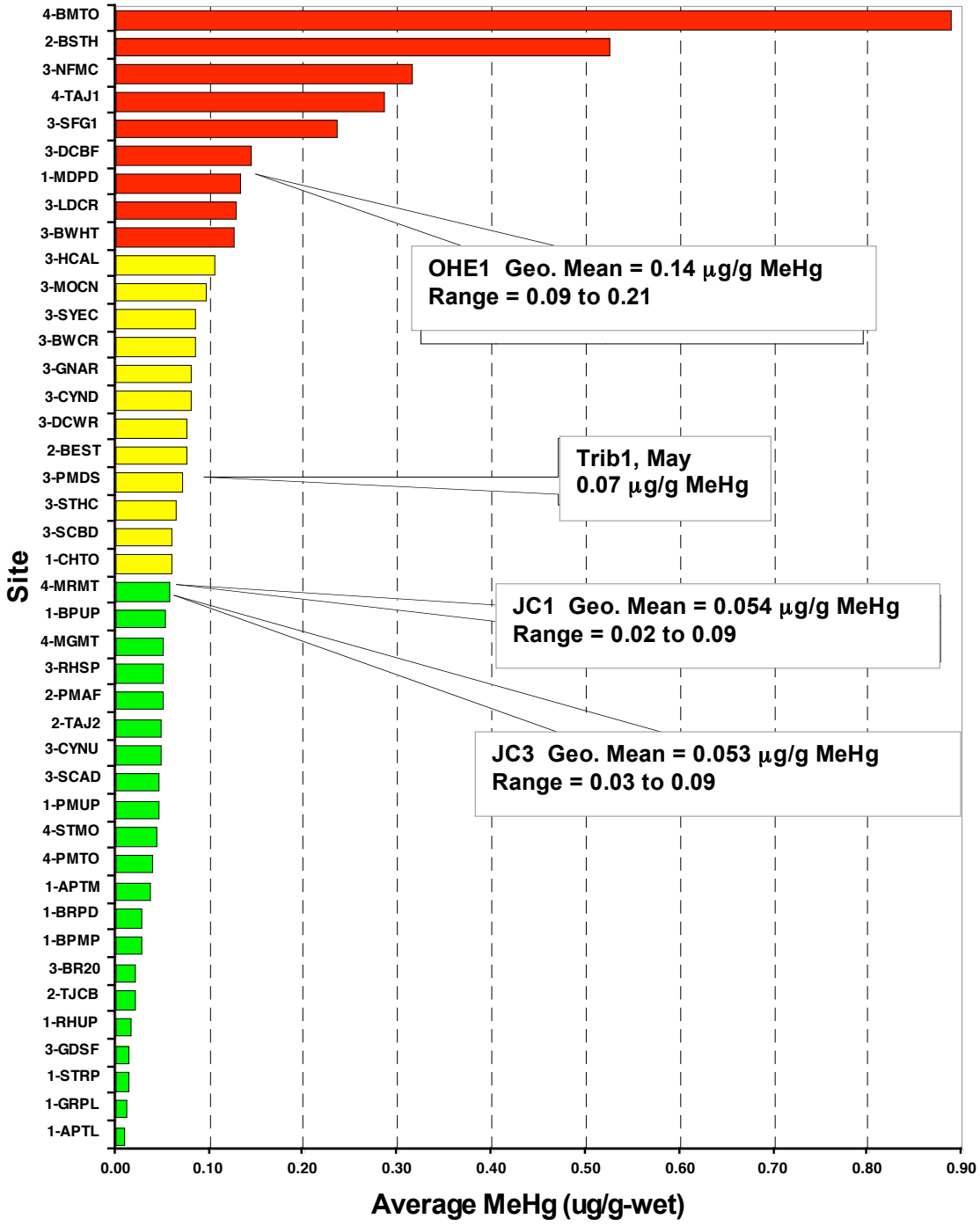

Figure 15. Average methylmercury concentration (µg/g, wet wt.) in larval dragonflies (Odonata) from 42 Sierra Nevada sites, 1999-2002, compared with selected water striders from the Oat Hill/James Creek study area, 2004. Methyl mercury in Sierra dragonflies was considered high (red), medium (yellow), or low (green) based on a comparison with the median for all sites. High: > 2 times the median, Medium: < 2 times the median, but greater than the median, and Low: less than the median.

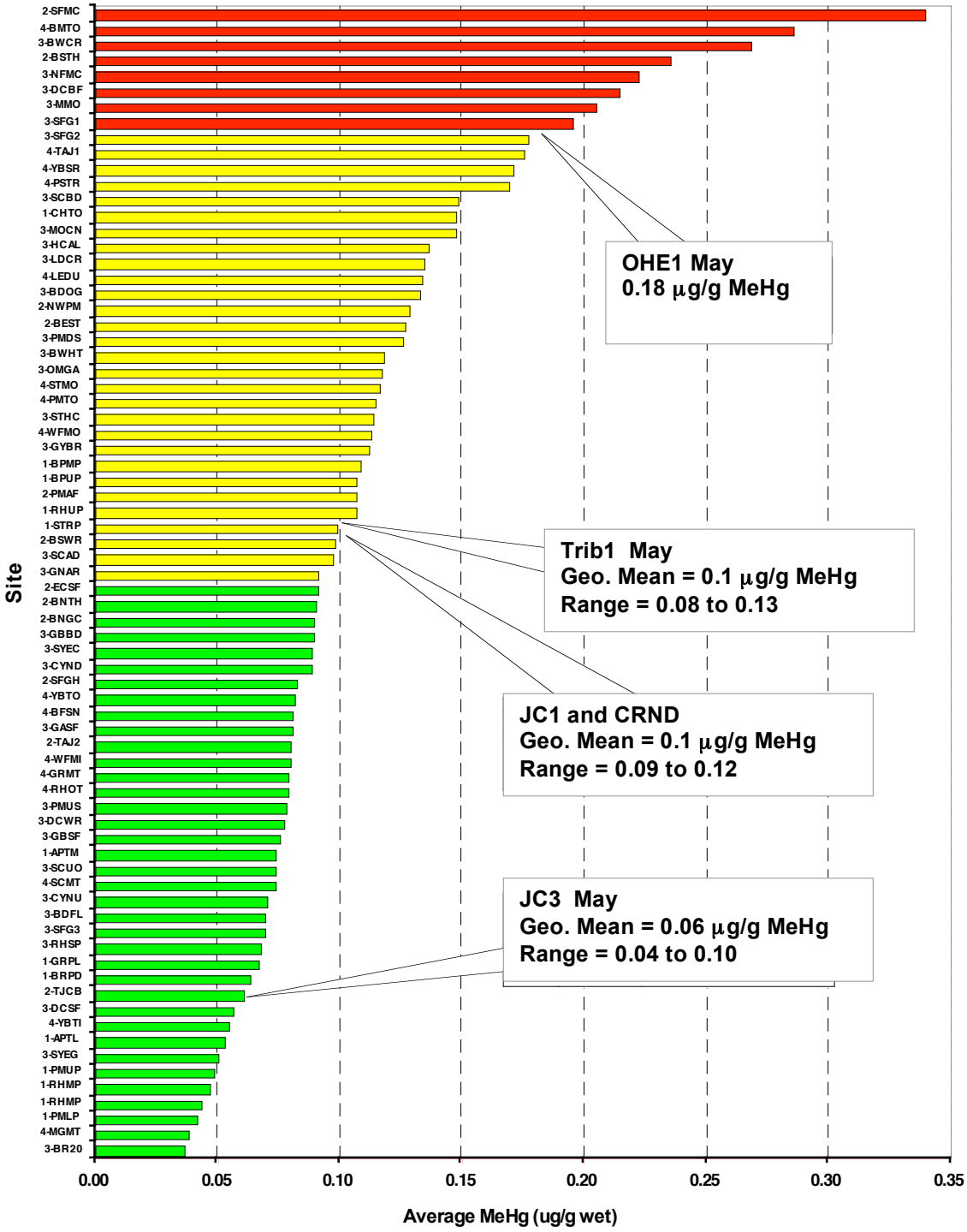

Figure 16. Average methylmercury concentration (µg/g, wet wt.) in adult water striders (Gerridae) from 74 Sierra Nevada sites, 1999-2002, compared with selected water striders from the Oat Hill/James Creek study area, 2004. Methyl mercury in Sierra water striders was considered high (red), medium (yellow), or low (green) based on a comparison with the median for all sites. High: > 2 times the median, Medium: < 2 times the median, but greater than the median, and Low: less than the median.

Table 2. Chemical analysis of tailings and sediments at the Oat Hill Extension site, and soil deemed as representing background concentrations.

	Lat	Long	Hg ppm	Ag ppm	Al %	As ppm	Ba ppm	Be ppm	Bi ppm	Ca %	Cd ppm	Ce ppm	Co ppm	Cr ppm	Cs ppm	Cu ppm	Fe %	Ga ppm	Ge ppm	Hf ppm	In ppm	K %	La ppm	Li ppm
Lower Tailings Pile at the Oat Hill Extension Mine																								
23-OE-1	38.67716	122.51748	767	0.17	6.4	5.2	750	1.4	0.2	1.8	0.2	44	16	91	5	36	3.9	14.0	0.3	1.5	0.03	1.6	22	32
23-OE-2	38.67813	122.5174	599	0.16	6.1	6.1	750	1.1	0.2	2.0	0.2	45	16	61	4	42	4.9	13.2	0.3	1	0.04	1.5	23	31
23-OE-4	38.67833	122.51745	827	0.16	6.1	3.2	700	1.3	0.1	1.9	0.1	48	15	92	4	32	4.3	13.3	0.3	1	0.04	1.5	24	31
23-OE-5	38.67833	122.51745	998	0.18	6.6	3.3	800	1.4	0.1	2.0	0.2	56	16	58	4	37	4.9	14.4	0.4	1.1	0.04	1.6	28	33
23-OE-6	38.67844	122.51781	891	0.15	5.9	4.4	720	1.2	0.1	2.0	0.2	48	16	96	4	38	4.5	13.0	0.3	1.1	0.03	1.5	24	29
23-OE-7	38.6784	122.51772	430	0.16	5.6	1.9	710	1.4	0.1	2.5	0.2	53	17	56	4	40	5.8	12.5	0.3	1.2	0.03	1.4	27	32
23-OE-8	38.67853	122.51758	830	0.15	5.5	0.2	610	1.1	0.1	1.9	0.2	49	14	87	4	31	4.9	12.0	0.3	1.4	0.03	1.3	25	34
23-OE-9	38.6787	122.51777	731	0.17	7.2	5.2	840	1.5	0.2	2.0	0.2	46	18	57	5	48	4.9	15.4	0.3	1.5	0.05	1.8	23	39
23-OE-10	38.67856	122.51746	403	0.1	5.1	<0.2	790	0.6	0.0	19.8	0.1	21	20	220	1	18	2.4	9.8	0.3	1.8	0.04	0.3	12	32
Upper Tailings above Adit at the Oat Hill Extension Mine																								
23-OE-12	38.6791	122.51866	1175	0.14	6.6	1.9	610	1.2	0.1	2.0	0.1	41	14	86	4	28	3.5	13.6	0.3	1.3	0.03	1.4	21	33
Sediments in Drainage A that transects the Oat Hill Extension Tailngs Pile																								
23-OE-13S	38.6791	122.51866	930	0.18	8.3	11.6	910	1.6	0.4	1.0	0.2	42	19	78	5	60	4.1	18.2	0.3	1.2	0.05	2.1	21	34
23-OE-3S	38.67813	122.5174	1495	0.18	7.5	9.3	880	1.2	0.2	1.2	0.2	44	21	73	4	63	4.7	16.5	0.3	1.1	0.06	1.9	22	31
Sample of retort brick at Oat Hill Extension Mine																								
23-OE-11	38.67846	122.51814	5.21	0.15	8.6	5.6	750	1.3	0.1	1.7	0.1	41	19	138	4	44	5.2	18.9	0.2	1.4	0.06	1.8	24	32
Background soil sample at Oat Hill Extension Office Site																								
23-OE-14	38.67752	122.51819	6.71	0.13	7.3	8	750	1.3	0.1	0.3	0.2	45	16	62	4	36	4.5	16.2	0.2	0.7	0.05	1.57	23	38

Screening criteria, in mg/kg (ppm)

BLM Camper	40			700			20					70						5000						
BLM Eco Risk	1						4					0.3						7						
EPA PRG	23			390		76000	22			5400	150	37			4700	210		2900			23000			
23-OE-1	+	+	+	-	-	-	-	+	-	-	-	-	-	-	-	-		-	+	-	-			
23-OE-2	+	+	+	-	-	-	-	+	-	-	-	-	-	-	-	-		-	+	-	-			
23-OE-4	+	+	+	-	-	-	-	-	-	-	-	-	-	-	-	-		-	+	-	-			
23-OE-5	+	+	+	-	-	-	-	-	-	-	-	-	-	-	-	-		-	+	-	-			
23-OE-6	+	+	+	-	-	-	-	+	-	-	-	-	-	-	-	-		-	+	-	-			
23-OE-7	+	+	+	-	-	-	-	-	-	-	-	-	-	-	-	-		-	+	-	-			
23-OE-8	+	+	+	-	-	-	-	-	-	-	-	-	-	-	-	-		-	+	-	-			
23-OE-9	+	+	+	-	-	-	-	+	-	-	-	-	-	-	-	-		-	+	-	-			
23-OE-10	+	+	+	-	-	-	+	+	+	-	-	-	-	-	-	+		-	+	-	-			
23-OE-12	+	+	+	-	-	-	-	-	-	-	-	-	-	-	-	-		-	+	-	-			
23-OE-3S	+	+	+	-	-	-	-	+	-	-	-	-	-	-	-	-		-	+	-	-			
23-OE-13S	+	+	+	-	-	-	-	+	-	-	-	-	-	-	-	-		-	+	-	-			
23-OE-11	-	+	-	-	-	-	-	+	-	-	-	-	-	-	-	-		-	+	-	-			
23-OE-14	-	+	-	-	-	-	-	+	-	-	-	-	-	-	-	-		-	+	-	-			

Note: Plus (+) signs indicate exceedance of the criterion listed, while minus (-) signs indicate that the element's concentration was below the criterion.

Table 2 continued.

	Mn ppm	Mo ppm	Na %	Nb ppm	Ni ppm	P ppm	Pb ppm	Rb ppm	S %	Sb ppm	Se ppm	Sn ppm	Sr ppm	Ta ppm	Te ppm	Th ppm	Ti %	Tl ppm	U ppm	V ppm	W ppm	Y ppm	Zn ppm	Zr ppm
Lower Tailings Pile at the Oat Hill Extension Mine																								
23-OE-1	576	0.96	0.5	7	55	630	15	64	0.23	1.06	2	2.5	235	0.3	0.05	8	0.3	0.5	1.9	119	2	15	92	36
23-OE-2	741	0.95	0.4	5.5	57	680	15	60	0.08	1.28	1	2.2	252	0.2	<0.05	7	0.3	0.4	1.9	126	1.2	16	110	26
23-OE-4	668	0.79	0.4	5.3	54	660	14	59	0.11	1.02	1	2	217	0.2	<0.05	6	0.3	0.4	2.1	122	1.1	16	105	28
23-OE-5	713	0.85	0.6	5.4	61	870	14	62	0.17	0.93	1	2.1	464	0.2	<0.05	7	0.3	0.4	2.1	128	1.4	19	108	35
23-OE-6	644	0.87	0.5	5.5	62	660	15	58	0.12	0.91	2	1.7	223	0.2	<0.05	7	0.3	0.4	1.9	118	1	18	112	27
23-OE-7	827	0.91	0.2	5.5	66	630	16	55	0.11	0.87	1	2.3	289	0.1	<0.05	7	0.3	0.4	2	128	1	21	127	19
23-OE-8	720	0.83	0.3	5.7	58	590	15	53	0.15	0.72	1	1.6	202	0.2	<0.05	6	0.3	0.3	1.8	116	0.8	18	113	34
23-OE-9	808	1.25	0.1	7	62	750	16	72	0.17	1.11	2	2.1	263	0.4	<0.05	6	0.4	0.5	2.2	134	1	16	110	45
23-OE-10	702	0.18	0.7	3.2	104	390	10	11	0.04	0.21	2	1.6	1450	0.2	<0.05	4	0.2	0.1	2.7	80	0.3	10	50	48
Upper Tailings above Adit at the Oat Hill Extension Mine																								
23-OE-12	545	0.65	0.5	6.6	48	600	13	56	0.08	0.71	2	1.6	207	0.3	<0.05	7	0.3	0.4	1.6	114	1	14	87	40
Sediments in Drainage A that transects the Oat Hill Extension Tailngs Pile																								
23-OE-13S	575	1.07	0.6	7	68	850	27	82	0.08	1.15	1	6.5	168.5	0.2	0.08	8	0.4	0.5	1.7	144	1.4	14	120	37
23-OE-3S	690	0.89	0.6	6.6	68	840	23	73	0.11	1.1	2	2.1	170.5	0.2	<0.05	8	0.4	0.5	1.8	140	1.2	15	121	28
Sample of retort brick at Oat Hill Extension Mine																								
23-OE-11	946	0.73	1.0	7.7	82	830	14	86	0.01	0.77	1	2.1	113.5	0.3	<0.05	7	0.5	0.4	1.7	144	0.8	16	110	43
Background soil sample at Oat Hill Extension Office Site																								
23-OE-14	698	0.88	0.1	6.6	54	940	15	70	0.02	0.96	<1	1.8	81	0.1	<0.05	7	0.4	0.4	1.8	130	1.1	15	123	18

Screening criteria, in mg/kg (ppm)

BLM Camper	19000				2700			1000			50		700			130						40000		
BLM Eco Risk								6														43		
EPA PRG	1800				1600						31		390			5.2			550			23000		
23-OE-1	-	-			-	-		-	+		-	-	-	-		-	+		-			-	+	-
23-OE-2	-	-			-	-		-	+		-	-	-	-		-	+		-			-	+	-
23-OE-4	-	-			-	-		-	+		-	-	-	-		-	+		-			-	+	-
23-OE-5	-	-			-	-		-	+		-	-	-	-		-	+		-			-	+	-
23-OE-6	-	-			-	-		-	+		-	-	-	-		-	+		-			-	+	-
23-OE-7	-	-			-	-		-	+		-	-	-	-		-	+		-			-	+	-
23-OE-8	-	-			-	-		-	+		-	-	-	-		-	+		-			-	+	-
23-OE-9	-	-			-	-		-	+		-	-	-	-		-	+		-			-	+	-
23-OE-10	-	-			-	-		-	+		-	-	-	-		-	-		-			-	+	-
23-OE-12	-	-			-	-		-	+		-	-	-	-		-	+		-			-	+	-
23-OE-3S	-	-			-	-		-	+		-	-	-	-		-	+		-			-	+	-
23-OE-13S	-	-			-	-		-	+		-	-	-	-		-	+		-			-	+	-
23-OE-11	-	-			-	-		-	+		-	-	-	-		-	+		-			-	+	-
23-OE-14	-	-			-	-		-	+		-	-	+	+		-	+		-			-	+	-

Appendix 1. Thermodynamic Modeling Results

A1.1 Sample 04JC1

```
          Temperature =  14.3 C    Pressure =  1.013 bars
          pH =  8.400              log fO2 =   -0.699
          Eh =   0.7423 volts      pe =  13.0145
          Ionic strength      =    0.006416
          Activity of water   =    0.999995
          Solvent mass        =    0.999999 kg
          Solution mass       =    1.000274 kg
          Solution density    =    1.020    g/cm3
          Chlorinity          =    0.000141 molal
          Dissolved solids    =         274 mg/kg sol'n
          Rock mass           =    0.000000 kg
          Carbonate alkalinity=       57.09 mg/kg as CaCO3

 No minerals in system.
```

Aqueous species	molality	mg/kg sol'n	act. coef.	log act.
Mg++	0.001650	40.10	0.7376	-2.9146
HCO3-	0.001088	66.39	0.9213	-2.9989
SO4--	0.0008443	81.08	0.7166	-3.2182
SiO2(aq)	0.0004752	28.54	1.0017	-3.3224
O2(aq)	0.0003151	10.08	1.0017	-3.5008
Ca++	0.0003105	12.44	0.7275	-3.6462
Na+	0.0002381	5.473	0.9204	-3.6592
Cl-	0.0001405	4.981	0.9185	-3.8891
MgSO4	0.0001169	14.06	1.0000	-3.9323
K+	4.585e-005	1.792	0.9185	-4.3756
CaSO4	2.693e-005	3.665	1.0000	-4.5698
H3SiO4-	1.434e-005	1.363	0.9204	-4.8796
MgHCO3+	1.308e-005	1.115	0.9204	-4.9196
CO3--	1.245e-005	0.7467	0.7194	-5.0480
CO2(aq)	1.101e-005	0.4844	1.0000	-4.9582
F-	9.865e-006	0.1874	0.9195	-5.0424
MgCO3	7.121e-006	0.6002	1.0000	-5.1475
CaHCO3+	3.764e-006	0.3804	0.9225	-5.4594
CaCO3	2.831e-006	0.2833	1.0000	-5.5481
Fe(OH)3	1.383e-006	0.1478	1.0000	-5.8591
OH-	1.170e-006	0.01990	0.9195	-5.9681
MgH3SiO4+	8.082e-007	0.09648	0.9204	-6.1285
Mn++	7.964e-007	0.04374	0.7275	-6.2370
NaSO4-	6.720e-007	0.07998	0.9204	-6.2087
MgF+	6.390e-007	0.02766	0.9204	-6.2305
Al(OH)4-	5.505e-007	0.05229	0.9204	-6.2953
MgH2SiO4	3.851e-007	0.04559	1.0000	-6.4144
NaHCO3	3.669e-007	0.03081	1.0000	-6.4355
MnO4-	3.135e-007	0.03728	0.9204	-6.5398
MgCl+	2.855e-007	0.01706	0.9204	-6.5804
CaCl+	2.006e-007	0.01515	0.9204	-6.7337
MgOH+	1.986e-007	0.008202	0.9204	-6.7381
KSO4-	1.906e-007	0.02576	0.9204	-6.7558
CaH3SiO4+	8.519e-008	0.01151	0.9204	-7.1056
Fe(OH)4-	6.119e-008	0.007578	0.9204	-7.2494
MnSO4	5.603e-008	0.008458	1.0000	-7.2516
Mg2CO3++	5.155e-008	0.005597	0.7222	-7.4292
Mg(H3SiO4)2	5.042e-008	0.01081	1.0000	-7.2974
NaH3SiO4	4.210e-008	0.004971	1.0000	-7.3757
Fe(OH)2+	2.387e-008	0.002145	0.9204	-7.6581
CaF+	2.315e-008	0.001367	0.9204	-7.6715
MnCO3	2.181e-008	0.002506	1.0000	-7.6614
MnHCO3+	1.125e-008	0.001304	0.9204	-7.9850
NaCO3-	8.982e-009	0.0007453	0.9204	-8.0826
CaH2SiO4	6.029e-009	0.0008088	1.0000	-8.2197
Al(OH)3	5.409e-009	0.0004218	1.0000	-8.2669
CaOH+	4.816e-009	0.0002749	0.9204	-8.3534
H+	4.287e-009	4.320e-006	0.9285	-8.4000
MnOH+	1.768e-009	0.0001272	0.9204	-8.7885
Ca(H3SiO4)2	1.106e-009	0.0002547	1.0000	-8.9561
NaCl	5.582e-010	3.261e-005	1.0000	-9.2532
MnO4--	3.760e-010	4.471e-005	0.7166	-9.5695

NaF	2.207e-010	9.264e-006	1.0000	-9.6562
HSO4-	1.892e-010	1.836e-005	0.9204	-9.7591
H2SiO4--	1.746e-010	1.642e-005	0.7166	-9.9027
H6(H2SiO4)4--	1.664e-010	6.362e-005	0.7166	-9.9236
NaOH	1.476e-010	5.904e-006	1.0000	-9.8308
KCl	1.198e-010	8.926e-006	1.0000	-9.9217
MnF+	1.039e-010	7.678e-006	0.9204	-10.0195
MnCl+	5.152e-011	4.656e-006	0.9204	-10.3240
Al(OH)2+	4.624e-011	2.820e-006	0.9204	-10.3710
HF	4.405e-011	8.810e-007	1.0000	-10.3561
KOH	1.363e-011	7.644e-007	1.0000	-10.8656
Mg2OH+++	1.254e-011	8.228e-007	0.5039	-11.1992
Mn2(OH)3+	7.357e-012	1.183e-006	0.9204	-11.1694
Mn(OH)2	2.327e-012	2.069e-007	1.0000	-11.6332

Mineral saturation states

	log Q/K		log Q/K
Birnessite	62.0314s/sat	Corundum	-5.6814
Todorokite	53.8835s/sat	Analc-dehydr	-5.9301
Antigorite	23.5060s/sat	Tephroite	-6.3095
Nontronit-Mg	17.9904s/sat	Kieserite	-6.3415
Nontronit-Ca	17.8719s/sat	Kalicinite	-7.3269
Nontronit-K	17.3791s/sat	Monticellite	-7.3284
Nontronit-Na	17.2487s/sat	Ca2Si3O8^5/2H2O	-7.5949
Hematite	12.8693s/sat	Jarosite-K	-7.7439
Bixbyite	11.7912s/sat	Grossular	-7.9896
Hausmannite	10.7270s/sat	Manganosite	-8.1233
Pyrolusite	10.2973s/sat	Mirabilite	-8.9470
Andradite	8.4136s/sat	Sylvite	-9.1036
Clinoptil-K	7.5931s/sat	Halite	-9.1091
Clinoptil-Ca	6.5058s/sat	MHSH(Mg1.5)	-9.1485
Saponite-Mg	6.4073s/sat	Cordier^hydr	-9.2637
Saponite-Ca	6.2875s/sat	NaFeO2(c)	-9.3334
Goethite	5.9729s/sat	Hydromagnesite	-9.6083
Saponite-K	5.7911s/sat	Spinel	-9.6289
Talc	5.7784s/sat	Jarosite-Na	-9.6830
Manganite	5.7492s/sat	Cronstedt-7A	-10.0436
Saponite-Na	5.6643s/sat	Arcanite	-10.1025
Smectite-Reykjan	5.2879s/sat	Portlandite	-10.2674
Saponite-H	5.1288s/sat	Ca(OH)2(c)	-10.2674
Epidote-ord	4.9176s/sat	Thenardite	-10.2982
Epidote	4.9169s/sat	Gaylussite	-10.6330
Phengite	4.8676s/sat	Mg2Cl(OH)3^4H2O	-11.0770
Tremolite	4.7374s/sat	Pirssonite	-11.2014
Ferrite-Mg	4.6942s/sat	Ca-Al Pyroxene	-11.5126
Clinochl-14A	4.3247s/sat	MgSO4(c)	-11.7262
Phlogopite	4.1606s/sat	Cordier^anhy	-11.8580
Muscovite	4.0978s/sat	Alunite	-11.9142
Heulandite	3.8585s/sat	KNaCO3^6H2O	-12.0369
Mordenite-K	3.7969s/sat	Ferrosilite	-12.4965
Ferrite-Ca	3.6283s/sat	MnSO4(c)	-12.5243
Sepiolite	3.4883s/sat	Siderite	-12.7491
Illite	3.3986s/sat	FeO(c)	-13.3426
Beidellit-Mg	3.0448s/sat	Wustite	-13.4707
Beidellit-Ca	2.9264s/sat	Akermanite	-13.5386
Clinoptil-Mg	2.6546s/sat	FeF3(c)	-14.1988
Maximum Microcli	2.5272s/sat	Mercallite	-14.3171
K-feldspar	2.5256s/sat	Kainite	-14.3472
Beidellit-K	2.4300s/sat	Bloedite	-14.4061
Pyrophyllite	2.4238s/sat	Fe(OH)2(ppd)	-14.8048
Kaolinite	2.3948s/sat	Hedenbergite	-15.1280
Beidellit-Na	2.3031s/sat	MgOHCl	-15.2249
Chrysotile	2.0032s/sat	Ca2SiO4^7/6H2O	-15.2640
Laumontite	1.9559s/sat	Bischofite	-15.3237
Beidellit-H	1.7649s/sat	Antarcticite	-15.4917
Clinoptil-Na	1.6297s/sat	Hercynite	-15.5839
Fe(OH)3(ppd)	1.4635s/sat	Na2Si2O5	-15.6939
Amesite-14A	1.3535s/sat	Ca2SiO4(gamma)	-15.9706
Dolomite	1.3528s/sat	Pargasite	-16.1825
Dolomite-ord	1.3528s/sat	CaCl2^4H2O	-16.3744
Sanidine high	1.2550s/sat	K2CO3^3/2H2O	-16.5364
Smectite-low-Fe-	0.9025s/sat	Na2SiO3	-16.6765
Quartz	0.8814s/sat	MnCl2^4H2O	-16.7940
Clinochl-7A	0.8620s/sat	Larnite	-17.5003
Mordenite-Na	0.8122s/sat	MnCl2^2H2O	-18.2097

Tridymite	0.7053s/sat	MgCl2^4H2O	-18.4317
Paragonite	0.6909s/sat	Melanterite	-18.9253
Magnetite	0.6812s/sat	Ripidolit-14A	-19.2978
Chalcedony	0.6000s/sat	Gehlenite	-19.3793
Cristobalite	0.3060s/sat	CaCl2^2H2O	-19.8055
Gibbsite	0.1088s/sat	Ferrite-2-Ca	-19.8335
Albite low	0.0447s/sat	Ca5Si6O17^21/2H2	-19.8387
Albite	0.0446s/sat	MnCl2^H2O	-19.8629
Calcite	-0.1090	CaCl2^H2O	-19.9904
Magnesite	-0.2345	Lime	-20.8108
Dolomite-dis	-0.2722	Rankinite	-21.1398
Aragonite	-0.2751	Ca5Si6O17^11/2H2	-22.0555
Lawsonite	-0.3166	Ripidolit-7A	-22.7633
Anthophyllite	-0.4425	Scacchite	-23.2493
Amrph^silica	-0.4939	Carnallite	-23.3558
Rhodochrosite	-0.7202	Hydrophilite	-23.7580
Diaspore	-0.7786	MgCl2^2H2O	-24.1788
Analcime	-1.0252	Merwinite	-24.3629
Monohydrocalcite	-1.0822	Chamosite-7A	-24.3692
Mn(OH)3(c)	-1.1293	FeSO4(c)	-24.4838
Albite high	-1.3464	Ca4Si3O10^3/2H2O	-24.5444
Enstatite	-1.4613	Na3H(SO4)2	-24.5479
Diopside	-1.4682	Ca2Cl2(OH)2^H2O	-25.1677
Prehnite	-1.5086	Ca5Si6O17^3H2O	-26.0551
Boehmite	-1.6806	Fayalite	-26.1180
Smectite-high-Fe	-1.7432	FeF2(c)	-26.1333
Gypsum	-2.4084	MgCl2^H2O	-27.7091
Jadeite	-2.4594	Ca3Si2O7^3H2O	-29.5057
Kalsilite	-2.5336	Minnesotaite	-32.0173
Huntite	-2.6292	Burkeite	-32.0252
Fluorite	-2.6313	Annite	-32.7742
Anhydrite	-2.6922	KMgCl3^2H2O	-33.5842
Wairakite	-2.8027	Chloromagnesite	-33.7243
Rhodonite	-2.9202	Greenalite	-34.4342
Dawsonite	-3.0874	Lawrencite	-35.5295
Brucite	-3.2864	Ca6Si6O18^H2O	-36.8727
Nesquehonite	-3.2982	Ca4Cl2(OH)6^13H2	-40.5750
Bassanite	-3.3239	Ca3SiO5	-40.7384
CaSO4^1/2H2O(bet	-3.5060	KMgCl3	-41.2551
CaSi2O5^2H2O	-3.5910	Molysite	-44.4385
Kyanite	-3.6532	Al2(SO4)3^6H2O	-46.1328
Andalusite	-3.9563	Fe2(SO4)3(c)	-48.6428
Margarite	-4.1204	Tachyhydrite	-50.7852
Epsomite	-4.2556	Na4SiO4	-52.9174
Wollastonite	-4.2974	Daphnite-14A	-55.4939
Sillimanite	-4.3366	Daphnite-7A	-58.9655
Clinozoisite	-4.3576	K8H4(CO3)6^3H2O	-62.1921
Zoisite	-4.4048	Al2(SO4)3	-64.6102
Artinite	-4.4182	Graphite	-78.4476
Hexahydrite	-4.5715	Na6Si2O7	-83.0656
Pseudowollastoni	-4.7137	Misenite	-95.0075
Nepheline	-4.8690	Sulfur-Rhmb	-111.9342
Pentahydrite	-4.8978	Alabandite	-146.2425
MgF2(c)	-4.9218	Pyrrhotite	-148.3603
Forsterite	-5.0606	Troilite	-154.6743
Anorthite	-5.0644	Pyrite	-255.7272
Mn(OH)2(am)	-5.3707	O-phth acid(c)	-618.8118
Leonhardtite	-5.4270		

Gases	fugacity	log fug.
O2(g)	0.2000	-0.699
Steam	0.01600	-1.796
CO2(g)	0.0002275	-3.643
H2(g)	8.245e-044	-43.084
H2S(g)	9.329e-150	-149.030
CH4(g)	3.843e-152	-151.415
S2(g)	2.451e-239	-238.611

Original basis	total moles	In fluid moles	mg/kg
Al+++	5.56e-007	5.56e-007	0.0150
Ca++	0.000344	0.000344	13.8
Cl-	0.000141	0.000141	5.00

F-	1.05e-005	1.05e-005	0.200
Fe++	1.47e-006	1.47e-006	0.0820
H+	-3.51e-005	-3.51e-005	-0.0354
H2O	55.5	55.5	1.00e+006
HCO3-	0.00114	0.00114	69.5
K+	4.60e-005	4.60e-005	1.80
Mg++	0.00179	0.00179	43.5
Mn++	1.20e-006	1.20e-006	0.0660
Na+	0.000239	0.000239	5.50
O2(aq)	0.000316	0.000316	10.1
SO4--	0.000989	0.000989	95.0
SiO2(aq)	0.000491	0.000491	29.5

Elemental composition	total moles	In fluid moles	mg/kg
Aluminum	5.559e-007	5.559e-007	0.01500
Calcium	0.0003443	0.0003443	13.80
Carbon	0.001139	0.001139	13.68
Chlorine	0.0001410	0.0001410	4.999
Fluorine	1.053e-005	1.053e-005	0.1999
Hydrogen	111.0	111.0	1.119e+005
Iron	1.468e-006	1.468e-006	0.08198
Magnesium	0.001790	0.001790	43.49
Manganese	1.201e-006	1.201e-006	0.06598
Oxygen	55.52	55.52	8.880e+005
Potassium	4.604e-005	4.604e-005	1.800
Silicon	0.0004910	0.0004910	13.79
Sodium	0.0002392	0.0002392	5.498
Sulfur	0.0009890	0.0009890	31.70

A1.2 Sample 04JC2

Temperature = 15.6 C Pressure = 1.013 bars
pH = 8.200 log fO2 = -0.699
Eh = 0.7513 volts pe = 13.1138
Ionic strength = 0.006656
Activity of water = 0.999995
Solvent mass = 1.000000 kg
Solution mass = 1.000284 kg
Solution density = 1.019 g/cm3
Chlorinity = 0.000144 molal
Dissolved solids = 283 mg/kg sol'n
Rock mass = 0.000000 kg
Carbonate alkalinity= 83.58 mg/kg as CaCO3

No minerals in system.

Aqueous species	molality	mg/kg sol'n	act. coef.	log act.
HCO3-	0.001602	97.71	0.9199	-2.8316
Mg++	0.001366	33.19	0.7338	-2.9989
Ca++	0.0008142	32.62	0.7234	-3.2299
SO4--	0.0005904	56.70	0.7122	-3.3762
Na+	0.0003378	7.765	0.9190	-3.5080
O2(aq)	0.0003074	9.833	1.0018	-3.5116
SiO2(aq)	0.0002819	16.93	1.0018	-3.5492
Cl-	0.0001431	5.072	0.9171	-3.8820
MgSO4	6.745e-005	8.116	1.0000	-4.1710
CaSO4	4.922e-005	6.699	1.0000	-4.3078
K+	4.845e-005	1.894	0.9171	-4.3523
CO2(aq)	2.518e-005	1.108	1.0000	-4.5990
MgHCO3+	1.592e-005	1.358	0.9190	-4.8347
CaHCO3+	1.450e-005	1.466	0.9212	-4.8742
CO3--	1.194e-005	0.7164	0.7151	-5.0685
F-	9.925e-006	0.1885	0.9180	-5.0404
CaCO3	7.173e-006	0.7178	1.0000	-5.1443
MgCO3	5.761e-006	0.4856	1.0000	-5.2395
H3SiO4-	5.608e-006	0.5332	0.9190	-5.2879
OH-	8.247e-007	0.01402	0.9180	-6.1209
NaHCO3	7.444e-007	0.06252	1.0000	-6.1282
NaSO4-	6.668e-007	0.07936	0.9190	-6.2127
Al(OH)4-	6.211e-007	0.05899	0.9190	-6.2435
MgF+	5.401e-007	0.02338	0.9190	-6.3042

CaCl+	5.170e-007	0.03904	0.9190	-6.3232
MgH3SiO4+	2.495e-007	0.02978	0.9190	-6.6396
MgCl+	2.341e-007	0.01399	0.9190	-6.6673
KSO4-	1.404e-007	0.01898	0.9190	-6.8892
MgOH+	1.169e-007	0.004829	0.9190	-6.9688
CaH3SiO4+	8.328e-008	0.01125	0.9190	-7.1162
MgH2SiO4	7.490e-008	0.008866	1.0000	-7.1255
CaF+	6.217e-008	0.003672	0.9190	-7.2431
Mg2CO3++	3.370e-008	0.003659	0.7179	-7.6163
NaH3SiO4	2.322e-008	0.002741	1.0000	-7.6341
Mn++	1.643e-008	0.0009025	0.7234	-7.9249
NaCO3-	1.177e-008	0.0009769	0.9190	-7.9658
CaOH+	8.946e-009	0.0005106	0.9190	-8.0850
Al(OH)3	8.852e-009	0.0006903	1.0000	-8.0530
H+	6.803e-009	6.855e-006	0.9274	-8.2000
Mg(H3SiO4)2	5.817e-009	0.001248	1.0000	-8.2353
CaH2SiO4	3.713e-009	0.0004981	1.0000	-8.4303
MnO4-	1.985e-009	0.0002360	0.9190	-8.7389
NaCl	8.282e-010	4.839e-005	1.0000	-9.0819
MnSO4	8.180e-010	0.0001235	1.0000	-9.0872
MnCO3	4.149e-010	4.768e-005	1.0000	-9.3820
Ca(H3SiO4)2	4.041e-010	9.305e-005	1.0000	-9.3935
MnHCO3+	3.415e-010	3.958e-005	0.9190	-9.5034
NaF	3.210e-010	1.347e-005	1.0000	-9.4935
HSO4-	2.159e-010	2.095e-005	0.9190	-9.7025
NaOH	1.474e-010	5.894e-006	1.0000	-9.8315
KCl	1.311e-010	9.767e-006	1.0000	-9.8826
Al(OH)2+	1.077e-010	6.570e-006	0.9190	-10.0043
HF	7.174e-011	1.435e-006	1.0000	-10.1442
H2SiO4--	4.749e-011	4.468e-006	0.7122	-10.4708
MnOH+	2.544e-011	1.830e-006	0.9190	-10.6311
KOH	1.016e-011	5.699e-007	1.0000	-10.9930
H6(H2SiO4)4--	8.252e-012	3.155e-006	0.7122	-11.2308
Mg2OH+++	6.082e-012	3.990e-007	0.4981	-11.5186
MnF+	2.194e-012	1.621e-007	0.9190	-11.6955
MnO4--	1.601e-012	1.903e-007	0.7122	-11.9430
MnCl+	1.076e-012	9.726e-008	0.9190	-12.0047

Mineral saturation states

	log Q/K		log Q/K
Birnessite	45.3285s/sat	MgF2(c)	-4.9899
Todorokite	39.2685s/sat	Anorthite	-5.0920
Antigorite	9.4467s/sat	Pentahydrite	-5.1401
Pyrolusite	8.1982s/sat	Rhodonite	-5.1802
Bixbyite	7.6590s/sat	Anthophyllite	-5.2332
Clinoptil-K	5.0927s/sat	Corundum	-5.2998
Hausmannite	4.5699s/sat	Leonhardtite	-5.6513
Clinoptil-Ca	4.4318s/sat	Forsterite	-6.0857
Saponite-Mg	4.2496s/sat	Analc-dehydr	-6.2539
Saponite-Ca	4.2100s/sat	Kieserite	-6.5443
Muscovite	3.6850s/sat	Kalicinite	-7.1839
Manganite	3.6613s/sat	Mn(OH)2(am)	-7.3784
Saponite-K	3.6433s/sat	Monticellite	-7.8615
Saponite-Na	3.5628s/sat	Grossular	-8.1061
Talc	3.5494s/sat	Ca2Si3O8^5/2H2O	-8.1654
Phengite	3.4498s/sat	Mirabilite	-8.8628
Saponite-H	3.0427s/sat	Halite	-8.9550
Illite	2.7092s/sat	Sylvite	-9.0885
Mordenite-K	2.5466s/sat	MHSH(Mg1.5)	-9.5347
Heulandite	2.5389s/sat	Spinel	-9.6290
Beidellit-Mg	2.4615s/sat	Gaylussite	-10.0732
Beidellit-Ca	2.4231s/sat	Manganosite	-10.1164
Kaolinite	2.2292s/sat	Portlandite	-10.1462
Phlogopite	2.1912s/sat	Ca(OH)2(c)	-10.1462
Clinochl-14A	1.8902s/sat	Thenardite	-10.1548
Beidellit-K	1.8564s/sat	Arcanite	-10.2363
Maximum Microcli	1.7760s/sat	Hydromagnesite	-10.3275
Beidellit-Na	1.7759s/sat	Cordier^hydr	-10.5397
K-feldspar	1.7746s/sat	Tephroite	-10.5799
Pyrophyllite	1.7682s/sat	Pirssonite	-10.5916
Dolomite	1.6648s/sat	Alunite	-11.1851
Dolomite-ord	1.6648s/sat	Ca-Al Pyroxene	-11.2679
Laumontite	1.3833s/sat	Mg2Cl(OH)3^4H2O	-11.7805
Beidellit-H	1.2527s/sat	MgSO4(c)	-11.8979
Tremolite	0.8826s/sat	KNaCO3^6H2O	-12.0086

Quartz	0.6299s/sat	Cordier^anhy	-13.1200
Sanidine high	0.5129s/sat	Akermanite	-14.2061
Tridymite	0.4551s/sat	Mercallite	-14.2902
Paragonite	0.4324s/sat	MnSO4(c)	-14.3210
Chalcedony	0.3498s/sat	Bloedite	-14.5039
Sepiolite	0.3345s/sat	Kainite	-14.5524
Calcite	0.2931s/sat	Antarcticite	-15.0673
Chrysotile	0.2803s/sat	Ca2SiO4^7/6H2O	-15.2902
Gibbsite	0.2727s/sat	Bischofite	-15.3815
Aragonite	0.1272s/sat	MgOHCl	-15.4063
Clinoptil-Mg	0.1173s/sat	CaCl2^4H2O	-15.9372
Cristobalite	0.0575s/sat	Ca2SiO4(gamma)	-15.9843
Dolomite-dis	0.0497s/sat	Na2Si2O5	-16.1978
Amesite-14A	-0.0621	K2CO3^3/2H2O	-16.5580
Mordenite-Na	-0.2896	Na2SiO3	-16.9306
Magnesite	-0.3163	Larnite	-17.5056
Lawsonite	-0.3912	MnCl2^4H2O	-18.4592
Albite low	-0.5556	MgCl2^4H2O	-18.4674
Albite	-0.5557	Pargasite	-18.5273
Clinoptil-Na	-0.5735	Gehlenite	-19.0147
Diaspore	-0.6029	CaCl2^2H2O	-19.3402
Monohydrocalcite	-0.6821	CaCl2^H2O	-19.5190
Amrph^silica	-0.7344	MnCl2^2H2O	-19.8567
Analcime	-1.3734	Lime	-20.6368
Boehmite	-1.4977	Ca5Si6O17^21/2H2	-20.9138
Clinochl-7A	-1.5614	Rankinite	-21.2945
Prehnite	-1.7381	MnCl2^H2O	-21.4972
Albite high	-1.9378	Ca5Si6O17^11/2H2	-23.0862
Enstatite	-2.1025	Hydrophilite	-23.2644
Gypsum	-2.1519	Carnallite	-23.4036
Fluorite	-2.2288	MgCl2^2H2O	-24.1762
Diopside	-2.2771	Na3H(SO4)2	-24.2706
Anhydrite	-2.4226	Ca2Cl2(OH)2^H2O	-24.6508
Rhodochrosite	-2.4252	Ca4Si3O10^3/2H2O	-24.8654
Huntite	-2.4621	Scacchite	-24.8663
Dawsonite	-2.6258	Merwinite	-24.8998
Kalsilite	-2.7665	Ca5Si6O17^3H2O	-27.0506
Jadeite	-2.8086	MgCl2^H2O	-27.6845
Bassanite	-3.0540	Ca3Si2O7^3H2O	-29.6476
Mn(OH)3(c)	-3.1706	Burkeite	-31.5446
CaSO4^1/2H2O(bet	-3.2344	KMgCl3^2H2O	-33.5648
Wairakite	-3.3324	Chloromagnesite	-33.6678
Nesquehonite	-3.3668	Ca6Si6O18^H2O	-37.7169
Kyanite	-3.5302	Ca4Cl2(OH)6^13H2	-40.0655
Brucite	-3.6795	Ca3SiO5	-40.5581
Margarite	-3.8096	KMgCl3	-41.1906
Andalusite	-3.8299	Al2(SO4)3^6H2O	-45.0866
CaSi2O5^2H2O	-4.0093	Tachyhydrite	-50.4305
Sillimanite	-4.2075	Na4SiO4	-53.0881
Clinozoisite	-4.3885	K8H4(CO3)6^3H2O	-61.6640
Zoisite	-4.4354	Al2(SO4)3	-63.4383
Wollastonite	-4.4443	Graphite	-77.7269
Epsomite	-4.5050	Na6Si2O7	-83.4210
Hexahydrite	-4.8120	Misenite	-95.0248
Pseudowollastoni	-4.8574	Sulfur-Rhmb	-111.1877
Artinite	-4.9131	Alabandite	-147.3430
Nepheline	-4.9524	O-phth acid(c)	-613.1751

Gases	fugacity	log fug.
O2(g)	0.2000	-0.699
Steam	0.01739	-1.760
CO2(g)	0.0005389	-3.268
H2(g)	1.410e-043	-42.851
H2S(g)	8.576e-149	-148.067
CH4(g)	4.844e-151	-150.315
S2(g)	9.702e-238	-237.013

Original basis	total moles	In fluid moles	mg/kg
Al+++	6.30e-007	6.30e-007	0.0170
Ca++	0.000886	0.000886	35.5
Cl-	0.000144	0.000144	5.10
F-	1.05e-005	1.05e-005	0.200
H+	-9.34e-006	-9.34e-006	-0.00941
H2O	55.5	55.5	1.00e+006
HCO3-	0.00168	0.00168	103.
K+	4.86e-005	4.86e-005	1.90
Mg++	0.00146	0.00146	35.4
Mn++	2.00e-008	2.00e-008	0.00110
Na+	0.000339	0.000339	7.80
O2(aq)	0.000307	0.000307	9.83
SO4--	0.000708	0.000708	68.0
SiO2(aq)	0.000288	0.000288	17.3

Elemental composition	total moles	In fluid moles	mg/kg
Aluminum	6.301e-007	6.301e-007	0.01700
Calcium	0.0008857	0.0008857	35.49
Carbon	0.001683	0.001683	20.21
Chlorine	0.0001439	0.0001439	5.099
Fluorine	1.053e-005	1.053e-005	0.1999
Hydrogen	111.0	111.0	1.119e+005
Magnesium	0.001456	0.001456	35.39
Manganese	2.002e-008	2.002e-008	0.001100
Oxygen	55.52	55.52	8.880e+005
Potassium	4.860e-005	4.860e-005	1.899
Silicon	0.0002879	0.0002879	8.084
Sodium	0.0003393	0.0003393	7.798
Sulfur	0.0007079	0.0007079	22.69

A1.3 Sample 04JC3

Temperature =	14.2 C	Pressure =	1.013 bars
pH =	8.200	log fO2 =	-0.699
Eh =	0.7538 volts	pe =	13.2223
Ionic strength	=	0.006399	
Activity of water	=	0.999995	
Solvent mass	=	1.000000 kg	
Solution mass	=	1.000273 kg	
Solution density	=	1.020 g/cm3	
Chlorinity	=	0.000144 molal	
Dissolved solids	=	274 mg/kg sol'n	
Rock mass	=	0.000000 kg	
Carbonate alkalinity	=	58.39 mg/kg as CaCO3	

No minerals in system.

Aqueous species	molality	mg/kg sol'n	act. coef.	log act.
Mg++	0.001620	39.36	0.7379	-2.9226
HCO3-	0.001126	68.69	0.9214	-2.9840
SO4--	0.0008353	80.21	0.7169	-3.2227
SiO2(aq)	0.0004436	26.64	1.0017	-3.3523
Ca++	0.0003364	13.48	0.7278	-3.6112
O2(aq)	0.0003158	10.10	1.0017	-3.4999
Na+	0.0002425	5.573	0.9205	-3.6513
Cl-	0.0001433	5.081	0.9186	-3.8805
MgSO4	0.0001135	13.66	1.0000	-3.9450
K+	4.585e-005	1.792	0.9186	-4.3755
CaSO4	2.887e-005	3.929	1.0000	-4.5396
CO2(aq)	1.808e-005	0.7955	1.0000	-4.7428
MgHCO3+	1.328e-005	1.133	0.9205	-4.9128
F-	9.875e-006	0.1876	0.9196	-5.0419
H3SiO4-	8.415e-006	0.8001	0.9205	-5.1109
CO3--	8.105e-006	0.4863	0.7197	-5.2341
MgCO3	4.544e-006	0.3830	1.0000	-5.3425
CaHCO3+	4.219e-006	0.4265	0.9226	-5.4097
CaCO3	1.996e-006	0.1997	1.0000	-5.6998
Fe(OH)3	1.900e-006	0.2030	1.0000	-5.7212
Al(OH)4-	7.369e-007	0.07000	0.9205	-6.1686

OH-	7.323e-007	0.01245	0.9196	-6.1718
Mn++	6.820e-007	0.03746	0.7278	-6.3042
NaSO4-	6.769e-007	0.08057	0.9205	-6.2054
MgF+	6.271e-007	0.02715	0.9205	-6.2387
MgH3SiO4+	4.673e-007	0.05578	0.9205	-6.3664
NaHCO3	3.874e-007	0.03253	1.0000	-6.4119
MgCl+	2.864e-007	0.01711	0.9205	-6.5790
CaCl+	2.223e-007	0.01679	0.9205	-6.6891
KSO4-	1.887e-007	0.02549	0.9205	-6.7603
MgH2SiO4	1.405e-007	0.01663	1.0000	-6.8523
MgOH+	1.218e-007	0.005032	0.9205	-6.9502
MnO4-	6.640e-008	0.007895	0.9205	-7.2138
CaH3SiO4+	5.437e-008	0.007349	0.9205	-7.3006
Fe(OH)4-	5.283e-008	0.006543	0.9205	-7.3131
Fe(OH)2+	5.226e-008	0.004695	0.9205	-7.3178
MnSO4	4.742e-008	0.007159	1.0000	-7.3240
Mg2CO3++	3.235e-008	0.003513	0.7225	-7.6313
NaH3SiO4	2.517e-008	0.002972	1.0000	-7.5991
CaF+	2.507e-008	0.001481	0.9205	-7.6368
Mg(H3SiO4)2	1.717e-008	0.003682	1.0000	-7.7652
MnCO3	1.220e-008	0.001402	1.0000	-7.9137
Al(OH)3	1.156e-008	0.0009011	1.0000	-7.9372
MnHCO3+	9.965e-009	0.001155	0.9205	-8.0375
H+	6.795e-009	6.846e-006	0.9286	-8.2000
NaCO3-	5.973e-009	0.0004956	0.9205	-8.2598
CaOH+	3.263e-009	0.0001862	0.9205	-8.5224
CaH2SiO4	2.428e-009	0.0003257	1.0000	-8.6147
MnOH+	9.479e-010	6.818e-005	0.9205	-9.0592
NaCl	5.784e-010	3.380e-005	1.0000	-9.2377
Ca(H3SiO4)2	4.159e-010	9.575e-005	1.0000	-9.3810
HSO4-	2.960e-010	2.872e-005	0.9205	-9.5647
NaF	2.246e-010	9.428e-006	1.0000	-9.6486
Al(OH)2+	1.579e-010	9.629e-006	0.9205	-9.8376
KCl	1.220e-010	9.092e-006	1.0000	-9.9137
NaOH	9.405e-011	3.761e-006	1.0000	-10.0266
MnF+	8.892e-011	6.572e-006	0.9205	-10.0870
HF	6.977e-011	1.395e-006	1.0000	-10.1563
H2SiO4--	6.417e-011	6.036e-006	0.7169	-10.3372
H6(H2SiO4)4--	5.025e-011	1.921e-005	0.7169	-10.4434
MnO4--	5.000e-011	5.945e-006	0.7169	-10.4456
MnCl+	4.502e-011	4.068e-006	0.9205	-10.3826
KOH	8.526e-012	4.782e-007	1.0000	-11.0693
Mg2OH+++	7.557e-012	4.957e-007	0.5043	-11.4189
FeOH++	1.948e-012	1.419e-007	0.7225	-11.8515
Mn2(OH)3+	1.356e-012	2.181e-007	0.9205	-11.9037

Mineral saturation states

	log Q/K		log Q/K
Birnessite	58.2938s/sat	Analc-dehydr	-5.8496
Todorokite	50.6131s/sat	Forsterite	-5.9196
Nontronit-Mg	18.2118s/sat	Kieserite	-6.3570
Nontronit-Ca	18.1005s/sat	Jarosite-K	-6.7304
Nontronit-K	17.6028s/sat	Tephroite	-7.2840
Nontronit-Na	17.4746s/sat	Kalicinite	-7.3083
Hematite	13.1507s/sat	Monticellite	-8.1438
Antigorite	13.0965s/sat	Ca2Si3O8^5/2H2O	-8.4207
Bixbyite	10.8535s/sat	Grossular	-8.5218
Pyrolusite	9.8310s/sat	Manganosite	-8.5978
Hausmannite	9.3172s/sat	Jarosite-Na	-8.6492
Clinoptil-K	7.5771s/sat	Cordier^hydr	-8.9081
Andradite	7.4990s/sat	Mirabilite	-8.9310
Clinoptil-Ca	6.5202s/sat	Halite	-9.0922
Goethite	6.1137s/sat	Sylvite	-9.0938
Manganite	5.2820s/sat	MHSH(Mg1.5)	-9.3724
Saponite-Mg	5.1045s/sat	Spinel	-9.3817
Saponite-Ca	4.9920s/sat	NaFeO2(c)	-9.3912
Epidote-ord	4.8981s/sat	Cronstedt-7A	-9.5226
Epidote	4.8973s/sat	Arcanite	-10.1051
Muscovite	4.8126s/sat	Thenardite	-10.2868
Smectite-Reykjan	4.8103s/sat	Alunite	-10.3168
Ferrite-Mg	4.5581s/sat	Portlandite	-10.6406
Saponite-K	4.4906s/sat	Ca(OH)2(c)	-10.6406
Phengite	4.4746s/sat	Hydromagnesite	-10.8067
Talc	4.4247s/sat	Gaylussite	-10.9453
Saponite-Na	4.3660s/sat	Ca-Al Pyroxene	-11.2503

Heulandite	3.9570s/sat	Cordier^anhy	-11.5035
Saponite-H	3.8940s/sat	Pirssonite	-11.5176
Illite	3.8427s/sat	Mg2Cl(OH)3^4H2O	-11.6888
Mordenite-K	3.7889s/sat	MgSO4(c)	-11.7441
Beidellit-Mg	3.6490s/sat	KNaCO3^6H2O	-12.2054
Beidellit-Ca	3.5379s/sat	Ferrosilite	-12.3918
Ferrite-Ca	3.5362s/sat	Siderite	-12.3978
Beidellit-K	3.0365s/sat	MnSO4(c)	-12.5997
Kaolinite	3.0053s/sat	FeO(c)	-13.2100
Pyrophyllite	2.9772s/sat	Wustite	-13.3453
Phlogopite	2.9669s/sat	FeF3(c)	-13.4530
Beidellit-Na	2.9118s/sat	Mercallite	-14.1186
Clinochl-14A	2.8361s/sat	Kainite	-14.3514
Clinoptil-Mg	2.6232s/sat	Bloedite	-14.4072
Maximum Microcli	2.5755s/sat	Fe(OH)2(ppd)	-14.6720
K-feldspar	2.5740s/sat	Akermanite	-14.7548
Beidellit-H	2.4371s/sat	Hercynite	-14.7870
Laumontite	2.1390s/sat	Bischofite	-15.3153
Tremolite	1.7011s/sat	Hedenbergite	-15.4225
Sepiolite	1.6657s/sat	MgOHCl	-15.4316
Clinoptil-Na	1.6261s/sat	Antarcticite	-15.4391
Fe(OH)3(ppd)	1.6032s/sat	Ca2SiO4^7/6H2O	-16.0369
Paragonite	1.4115s/sat	Na2Si2O5	-16.1416
Sanidine high	1.3027s/sat	CaCl2^4H2O	-16.3228
Magnetite	1.0956s/sat	K2CO3^3/2H2O	-16.7187
Dolomite	1.0060s/sat	Ca2SiO4(gamma)	-16.7445
Dolomite-ord	1.0060s/sat	MnCl2^4H2O	-16.8446
Amesite-14A	0.9715s/sat	Na2SiO3	-17.0961
Quartz	0.8534s/sat	Pargasite	-17.9522
Smectite-low-Fe-	0.8257s/sat	MnCl2^2H2O	-18.2617
Mordenite-Na	0.8104s/sat	Larnite	-18.2750
Chrysotile	0.7053s/sat	Melanterite	-18.3904
Tridymite	0.6772s/sat	MgCl2^4H2O	-18.4251
Chalcedony	0.5719s/sat	Gehlenite	-19.4900
Gibbsite	0.4425s/sat	Ripidolit-14A	-19.6910
Cristobalite	0.2777s/sat	CaCl2^2H2O	-19.7559
Albite low	0.0991s/sat	MnCl2^H2O	-19.9160
Albite	0.0990s/sat	CaCl2^H2O	-19.9414
Lawsonite	-0.0770	Ferrite-2-Ca	-20.3039
Calcite	-0.2607	Lime	-21.1880
Aragonite	-0.4267	Ca5Si6O17^21/2H2	-21.8593
Magnesite	-0.4303	Rankinite	-22.3140
Diaspore	-0.4459	Ripidolit-7A	-23.1574
Amrph^silica	-0.5228	Scacchite	-23.3036
Dolomite-dis	-0.6198	Carnallite	-23.3372
Clinochl-7A	-0.6274	Chamosite-7A	-23.4651
Analcime	-0.9429	Hydrophilite	-23.7107
Rhodochrosite	-0.9737	FeSO4(c)	-23.9541
Monohydrocalcite	-1.2336	Ca5Si6O17^11/2H2	-24.0795
Albite high	-1.2927	MgCl2^2H2O	-24.1752
Boehmite	-1.3484	Na3H(SO4)2	-24.3285
Mn(OH)3(c)	-1.6001	Ca2Cl2(OH)2^H2O	-25.4860
Prehnite	-1.6683	FeF2(c)	-25.5968
Smectite-high-Fe	-1.8754	Fayalite	-25.8808
Enstatite	-1.9046	Merwinite	-25.9530
Diopside	-2.3098	Ca4Si3O10^3/2H2O	-26.1170
Jadeite	-2.3769	MgCl2^H2O	-27.7071
Gypsum	-2.3777	Ca5Si6O17^3H2O	-28.0818
Kalsilite	-2.4303	Ca3Si2O7^3H2O	-30.6810
Fluorite	-2.5940	Minnesotaite	-31.7289
Wairakite	-2.6229	Burkeite	-32.1658
Anhydrite	-2.6625	Annite	-32.3253
Dawsonite	-2.7295	KMgCl3^2H2O	-33.5708
Kyanite	-3.0176	Chloromagnesite	-33.7248
Margarite	-3.2180	Greenalite	-34.0894
Bassanite	-3.2943	Lawrencite	-34.9789
Andalusite	-3.3210	Ca6Si6O18^H2O	-39.2749
Huntite	-3.3691	KMgCl3	-41.2452
Rhodonite	-3.4216	Ca4Cl2(OH)6^13H2	-41.6202
CaSO4^1/2H2O(bet	-3.4766	Ca3SiO5	-41.8912
Nesquehonite	-3.4951	Molysite	-43.6771
Anthophyllite	-3.5697	Al2(SO4)3^6H2O	-44.2784
Brucite	-3.7015	Fe2(SO4)3(c)	-47.1812
Sillimanite	-3.7015	Tachyhydrite	-50.7194
CaSi2O5^2H2O	-4.0174	Na4SiO4	-53.7351
Clinozoisite	-4.1863	Daphnite-14A	-54.2443

Zoisite	-4.2335	Daphnite-7A	-57.7168
Epsomite	-4.2675	K8H4(CO3)6^3H2O	-62.4822
Hexahydrite	-4.5840	Al2(SO4)3	-62.7654
Wollastonite	-4.6973	Graphite	-78.2601
Nepheline	-4.7597	Na6Si2O7	-84.3083
Anorthite	-4.8284	Misenite	-93.8150
Pentahydrite	-4.9102	Sulfur-Rhmb	-111.5776
MgF2(c)	-4.9297	Alabandite	-146.3717
Corundum	-5.0184	Pyrrhotite	-147.8976
Artinite	-5.0275	Troilite	-154.1967
Pseudowollastoni	-5.1138	Pyrite	-254.8885
Leonhardtite	-5.4408	O-phth acid(c)	-617.3016
Mn(OH)2(am)	-5.8441		

Gases	fugacity	log fug.
O2(g)	0.2000	-0.699
Steam	0.01590	-1.799
CO2(g)	0.0003726	-3.429
H2(g)	7.910e-044	-43.102
H2S(g)	2.040e-149	-148.690
CH4(g)	5.532e-152	-151.257
S2(g)	1.243e-238	-237.906

Original basis	total moles	In fluid moles	mg/kg
Al+++	7.49e-007	7.49e-007	0.0202
Ca++	0.000372	0.000372	14.9
Cl-	0.000144	0.000144	5.10
F-	1.05e-005	1.05e-005	0.200
Fe++	2.01e-006	2.01e-006	0.112
H+	-1.39e-005	-1.39e-005	-0.0140
H2O	55.5	55.5	1.00e+006
HCO3-	0.00118	0.00118	71.8
K+	4.60e-005	4.60e-005	1.80
Mg++	0.00175	0.00175	42.6
Mn++	8.19e-007	8.19e-007	0.0450
Na+	0.000244	0.000244	5.60
O2(aq)	0.000316	0.000316	10.1
SO4--	0.000979	0.000979	94.0
SiO2(aq)	0.000453	0.000453	27.2

Elemental composition	total moles	In fluid moles	mg/kg
Aluminum	7.487e-007	7.487e-007	0.02019
Calcium	0.0003718	0.0003718	14.90
Carbon	0.001177	0.001177	14.13
Chlorine	0.0001439	0.0001439	5.099
Fluorine	1.053e-005	1.053e-005	0.1999
Hydrogen	111.0	111.0	1.119e+005
Iron	2.005e-006	2.005e-006	0.1120
Magnesium	0.001753	0.001753	42.59
Manganese	8.191e-007	8.191e-007	0.04499
Oxygen	55.52	55.52	8.880e+005
Potassium	4.604e-005	4.604e-005	1.800
Silicon	0.0004527	0.0004527	12.71
Sodium	0.0002436	0.0002436	5.598
Sulfur	0.0009786	0.0009786	31.36

A1.3 Sample 04OHE1

Temperature =	19.3 C	Pressure =	1.013 bars
pH =	8.300	log fO2 =	-0.699
Eh =	0.7387 volts	pe =	12.7316
Ionic strength	=	0.013425	
Activity of water	=	0.999995	
Solvent mass	=	1.000000 kg	
Solution mass	=	1.000405 kg	
Solution density	=	1.017 g/cm3	
Chlorinity	=	0.000127 molal	
Dissolved solids	=	405 mg/kg sol'n	
Rock mass	=	0.000000 kg	
Carbonate alkalinity=		58.89 mg/kg as CaCO3	

No minerals in system.

Aqueous species	molality	mg/kg sol'n	act. coef.	log act.
Mg++	0.004155	100.9	0.6631	-2.5599
HCO3-	0.001086	66.23	0.8926	-3.0135
Ca++	0.001075	43.05	0.6464	-3.1583
SO4--	0.0009844	94.52	0.6280	-3.2088
Na+	0.0005976	13.73	0.8909	-3.2737
O2(aq)	0.0002867	9.169	1.0035	-3.5411
MgSO4	0.0002793	33.60	1.0000	-3.5539
SiO2(aq)	0.0002671	16.04	1.0035	-3.5718
Cl-	0.0001259	4.462	0.8874	-3.9519
CaSO4	8.762e-005	11.92	1.0000	-4.0574
K+	6.367e-005	2.488	0.8874	-4.2480
MgHCO3+	3.011e-005	2.568	0.8909	-4.5715
MgCO3	1.530e-005	1.290	1.0000	-4.8152
F-	1.354e-005	0.2571	0.8892	-4.9195
CO2(aq)	1.253e-005	0.5514	1.0000	-4.9019
CO3--	1.205e-005	0.7228	0.6328	-5.1178
CaHCO3+	1.176e-005	1.188	0.8949	-4.9780
CaCO3	7.976e-006	0.7980	1.0000	-5.0982
H3SiO4-	7.778e-006	0.7395	0.8909	-5.1593
MgF+	2.146e-006	0.09287	0.8909	-5.7186
NaSO4-	1.767e-006	0.2103	0.8909	-5.8029
OH-	1.450e-006	0.02465	0.8892	-5.8896
MgH3SiO4+	8.453e-007	0.1009	0.8909	-6.1232
NaHCO3	7.814e-007	0.06562	1.0000	-6.1071
MgOH+	5.898e-007	0.02436	0.8909	-6.2794
MgCl+	5.323e-007	0.03179	0.8909	-6.3240
Al(OH)4-	5.180e-007	0.04920	0.8909	-6.3358
CaCl+	4.937e-007	0.03728	0.8909	-6.3567
MgH2SiO4	3.097e-007	0.03666	1.0000	-6.5091
KSO4-	2.736e-007	0.03697	0.8909	-6.6130
Mg2CO3++	2.605e-007	0.02828	0.6374	-6.7797
CaH3SiO4+	1.211e-007	0.01636	0.8909	-6.9672
CaF+	1.070e-007	0.006319	0.8909	-7.0208
NaH3SiO4	5.303e-008	0.006261	1.0000	-7.2754
Mn++	2.796e-008	0.001535	0.6464	-7.7430
Mg(H3SiO4)2	2.283e-008	0.004896	1.0000	-7.6414
CaOH+	1.917e-008	0.001094	0.8909	-7.7676
NaCO3-	1.699e-008	0.001409	0.8909	-7.8201
MnO4-	1.098e-008	0.001306	0.8909	-8.0094
CaH2SiO4	6.588e-009	0.0008836	1.0000	-8.1813
H+	5.534e-009	5.575e-006	0.9057	-8.3000
Al(OH)3	4.511e-009	0.0003517	1.0000	-8.3458
MnSO4	1.956e-009	0.0002952	1.0000	-8.7086
NaCl	1.315e-009	7.685e-005	1.0000	-8.8809
NaF	7.741e-010	3.249e-005	1.0000	-9.1112
Ca(H3SiO4)2	6.807e-010	0.0001567	1.0000	-9.1670
MnCO3	5.223e-010	6.002e-005	1.0000	-9.2820
NaOH	4.325e-010	1.729e-005	1.0000	-9.3640
MnHCO3+	3.578e-010	4.147e-005	0.8909	-9.4966
HSO4-	2.873e-010	2.787e-005	0.8909	-9.5919
KCl	1.500e-010	1.118e-005	1.0000	-9.8239
H2SiO4--	1.181e-010	1.110e-005	0.6280	-10.1299
Mg2OH+++	1.003e-010	6.582e-006	0.3962	-10.4006
HF	8.037e-011	1.607e-006	1.0000	-10.0949
MnOH+	6.726e-011	4.837e-006	0.8909	-10.2224
Al(OH)2+	3.325e-011	2.027e-006	0.8909	-10.5284
KOH	2.245e-011	1.259e-006	1.0000	-10.6488
MnO4--	1.444e-011	1.717e-006	0.6280	-11.0424
H6(H2SiO4)4--	1.204e-011	4.604e-006	0.6280	-11.1212
MnF+	4.856e-012	3.589e-007	0.8909	-11.3639
MnCl+	1.437e-012	1.298e-007	0.8909	-11.8928

Mineral saturation states

	log Q/K		log Q/K
Birnessite	48.3835s/sat	Clinozoisite	-4.8469
Todorokite	41.9416s/sat	Zoisite	-4.8929
Antigorite	28.3814s/sat	Nepheline	-4.9896
Pyrolusite	8.5484s/sat	Leonhardtite	-4.9943
Bixbyite	8.5443s/sat	Sillimanite	-5.0083
Saponite-Mg	6.4792s/sat	Margarite	-5.0382

Saponite-Ca	6.3723s/sat	Anorthite	-5.4923
Hausmannite	6.0132s/sat	Kieserite	-5.8259
Saponite-K	5.8020s/sat	Corundum	-6.0066
Saponite-Na	5.7760s/sat	Analc-dehydr	-6.3516
Talc	5.7453s/sat	Monticellite	-6.5198
Tremolite	5.4209s/sat	Mn(OH)2(am)	-6.7729
Saponite-H	5.1434s/sat	Kalicinite	-7.3944
Clinochl-14A	5.1122s/sat	Ca2Si3O8^5/2H2O	-7.4720
Phlogopite	4.3124s/sat	Hydromagnesite	-7.6040
Manganite	4.0432s/sat	Grossular	-7.6900
Clinoptil-K	3.8441s/sat	MHSH(Mg1.5)	-8.3319
Phengite	3.7381s/sat	Mirabilite	-8.3987
Clinoptil-Ca	3.2031s/sat	Halite	-8.8021
Sepiolite	3.1612s/sat	Sylvite	-9.0962
Chrysotile	2.6668s/sat	Spinel	-9.4096
Muscovite	2.4040s/sat	Tephroite	-9.4683
Dolomite	2.1408s/sat	Manganosite	-9.4693
Dolomite-ord	2.1408s/sat	Thenardite	-9.5199
Mordenite-K	1.9218s/sat	Portlandite	-9.5808
Illite	1.8010s/sat	Ca(OH)2(c)	-9.5808
Clinochl-7A	1.6915s/sat	Arcanite	-9.9213
Amesite-14A	1.6294s/sat	Gaylussite	-9.9600
Heulandite	1.5835s/sat	Pirssonite	-10.3371
Beidellit-Mg	1.3390s/sat	Mg2Cl(OH)3^4H2O	-10.5120
Maximum Microcli	1.3231s/sat	Cordier^hydr	-10.6076
K-feldspar	1.3219s/sat	MgSO4(c)	-11.0917
Beidellit-Ca	1.2327s/sat	Ca-Al Pyroxene	-11.5188
Kaolinite	1.2159s/sat	KNaCO3^6H2O	-12.0719
Laumontite	0.6825s/sat	Akermanite	-12.4016
Beidellit-K	0.6625s/sat	Alunite	-12.5244
Beidellit-Na	0.6364s/sat	Cordier^anhy	-13.1485
Pyrophyllite	0.6092s/sat	Bloedite	-13.2616
Dolomite-dis	0.5538s/sat	MnSO4(c)	-13.8322
Quartz	0.5388s/sat	Kainite	-13.8905
Tridymite	0.3677s/sat	Mercallite	-14.2246
Calcite	0.3359s/sat	Ca2SiO4^7/6H2O	-14.2986
Chalcedony	0.2622s/sat	MgOHCl	-14.6681
Anthophyllite	0.2228s/sat	Ca2SiO4(gamma)	-14.9574
Aragonite	0.1706s/sat	Bischofite	-15.0474
Magnesite	0.1403s/sat	Antarcticite	-15.1517
Sanidine high	0.0853s/sat	Pargasite	-15.1744
Beidellit-H	-0.0001	Na2Si2O5	-15.4413
Cristobalite	-0.0251	CaCl2^4H2O	-15.9855
Gibbsite	-0.1563	Na2SiO3	-16.0876
Clinoptil-Mg	-0.6369	Larnite	-16.4549
Paragonite	-0.6449	K2CO3^3/2H2O	-16.5310
Monohydrocalcite	-0.6461	MgCl2^4H2O	-18.0707
Mordenite-Na	-0.7258	MnCl2^4H2O	-18.3937
Amrph^silica	-0.7950	Gehlenite	-18.7037
Albite low	-0.8145	Ca5Si6O17^21/2H2	-19.1173
Albite	-0.8146	CaCl2^2H2O	-19.3096
Lawsonite	-0.9235	CaCl2^H2O	-19.4709
Diaspore	-0.9985	MnCl2^2H2O	-19.7396
Huntite	-1.0202	Rankinite	-19.8234
Diopside	-1.0946	Lime	-19.9232
Enstatite	-1.2897	Ca5Si6O17^11/2H2	-21.1644
Clinoptil-Na	-1.4453	MnCl2^H2O	-21.3440
Analcime	-1.5394	Merwinite	-22.5034
Prehnite	-1.8648	Ca4Si3O10^3/2H2O	-23.0211
Boehmite	-1.8733	Carnallite	-23.0913
Gypsum	-1.9160	Hydrophilite	-23.1538
Fluorite	-1.9630	Na3H(SO4)2	-23.4994
Anhydrite	-2.1497	MgCl2^2H2O	-23.6718
Albite high	-2.1716	Ca2Cl2(OH)2^H2O	-24.2505
Rhodochrosite	-2.2809	Scacchite	-24.6642
Mn(OH)3(c)	-2.6594	Ca5Si6O17^3H2O	-25.0297
Bassanite	-2.7802	MgCl2^H2O	-27.1184
Brucite	-2.7850	Ca3Si2O7^3H2O	-28.1410
Nesquehonite	-2.8798	Burkeite	-30.1022
CaSO4^1/2H2O(bet	-2.9560	Chloromagnesite	-33.0120
Jadeite	-2.9771	KMgCl3^2H2O	-33.0636
Kalsilite	-2.9946	Ca6Si6O18^H2O	-35.0458
Dawsonite	-3.0609	Ca3SiO5	-38.7615
Artinite	-3.6188	Ca4Cl2(OH)6^13H2	-39.2404
CaSi2O5^2H2O	-3.7290	KMgCl3	-40.5627
Wairakite	-3.9127	Al2(SO4)3^6H2O	-46.0578

Epsomite	-3.9196	Tachyhydrite	-49.7167
Wollastonite	-4.0165	Na4SiO4	-51.0701
Hexahydrite	-4.1994	K8H4(CO3)6^3H2O	-62.4544
MgF2(c)	-4.2728	Al2(SO4)3	-64.0564
Kyanite	-4.3481	Graphite	-77.0176
Forsterite	-4.3526	Na6Si2O7	-80.3655
Pseudowollastoni	-4.4209	Misenite	-94.4424
Pentahydrite	-4.5336	Sulfur-Rhmb	-109.8050
Andalusite	-4.6380	Alabandite	-144.9036
Rhodonite	-4.6672	O-phth acid(c)	-607.8719

Gases	fugacity	log fug.
O2(g)	0.2000	-0.699
Steam	0.02195	-1.659
CO2(g)	0.0002957	-3.529
H2(g)	6.339e-043	-42.198
H2S(g)	8.408e-147	-146.075
CH4(g)	2.870e-149	-148.542
S2(g)	1.110e-234	-233.955

		In fluid	
Original basis	total moles	moles	mg/kg
Al+++	5.23e-007	5.23e-007	0.0141
Ca++	0.00118	0.00118	47.4
Cl-	0.000127	0.000127	4.50
F-	1.58e-005	1.58e-005	0.300
H+	-3.67e-005	-3.67e-005	-0.0370
H2O	55.5	55.5	1.00e+006
HCO3-	0.00118	0.00118	71.8
K+	6.39e-005	6.39e-005	2.50
Mg++	0.00448	0.00448	109.
Mn++	4.19e-008	4.19e-008	0.00230
Na+	0.000600	0.000600	13.8
O2(aq)	0.000287	0.000287	9.17
SO4--	0.00135	0.00135	130.
SiO2(aq)	0.000276	0.000276	16.6

Elemental composition	total moles	In fluid moles	mg/kg
Aluminum	5.226e-007	5.226e-007	0.01409
Calcium	0.001183	0.001183	47.38
Carbon	0.001177	0.001177	14.13
Chlorine	0.0001269	0.0001269	4.498
Fluorine	1.579e-005	1.579e-005	0.2999
Hydrogen	111.0	111.0	1.119e+005
Magnesium	0.004485	0.004485	109.0
Manganese	4.187e-008	4.187e-008	0.002299
Oxygen	55.52	55.52	8.879e+005
Potassium	6.394e-005	6.394e-005	2.499
Silicon	0.0002763	0.0002763	7.756
Sodium	0.0006003	0.0006003	13.79
Sulfur	0.001353	0.001353	43.37